Title: Involvement of autophagy in hypoxic-excitotoxic neuronal death.

Authors: Ginet V, Spiehlmann A, Rummel C, Rudinskiy N, Grishchuk Y, Luthi-Carter R, Clarke PG, Truttmann AC, Puyal J

Journal: Autophagy

Year: 2014 May

Volume: 10

Issue: 5

Pages: 846-60

DOI: 10.4161/auto.28264

Involvement of autophagy in hypoxic-excitotoxic neuronal death

Vanessa Ginet[1], Amélie Spiehlmann[1], Coralie Rummel[1], Nikita Rudinskiy[2], Yulia Grishchuk[1], Ruth Luthi-Carter[2], Peter G.H. Clarke[1], Anita C. Truttmann[3] and Julien Puyal[1*]

[1]Department of Fundamental Neurosciences, Faculty of Biology and Medicine, University of Lausanne, Rue du Bugnon 9, CH-1005 Lausanne, Switzerland

[2]Brain Mind Institute, École Polytechnique Fédérale de Lausanne, Station 15, Lausanne CH1015, Switzerland

[3]Clinic of Neonatology, Department of Pediatrics and Pediatric Surgery, University Hospital Center and University of Lausanne, CH-1011 Lausanne, Switzerland

[*] To whom correspondence should be addressed:

JulienPierre.Puyal@unil.ch;

phone: +41 (0)21 692 5122; FAX: +41 (0)21 692 5255

Keywords: autophagy, neonatal hypoxia-ischemia, neuroprotection, neuronal death, excitotoxicity.

Acknowledgments: We thank the Cellular Imaging Facility (University of Lausanne, Switzerland) for experimental support. This research was supported by grants from the Swiss National Science Foundation (310030-130769), from the Fondation Emma Muschamp and from the Faculté de Biologie et de Médecine (Lausanne).

Abbreviations: Hx, hypoxia; HI, hypoxia-ischemia; Ka, Kainate; LAMP1, lysosomal-associated membrane protein 1; LC3, microtubule-associated protein 1 light chain 3; 3-MA, 3-methyladenine; PepA; pepstatin A; PI, propidium iodide; Q-VD-OPH, Quinoline-Val-Asp(ome)-Ch2-O-phenoxy; ROS, reactive oxygen species; shRNA, short hairpin RNA; STS, staurosporine.

Running title: autophagy in hypoxic-excitotoxic neuronal death

Conflict of Interest Statement: The authors declare no conflict of interest.

Abstract

Neuronal autophagy has been shown to be increased in numerous excitotoxic conditions including neonatal cerebral hypoxia-ischemia (HI). However the role of this HI-induced autophagy remains unclear. To clarify this role we established an *in vitro* model of excitotoxicity combining kainate treatment (Ka, 30μM) with hypoxia (Hx, 6% oxygen) in primary neuron cultures. KaHx rapidly induced excitotoxic death that was completely prevented by MK801 or EGTA. KaHx also stimulated neuronal autophagic flux as shown by a rise in autophagosome number (increased levels of LC3-II and punctate LC3 labeling) accompanied by increases in lysosomal abundance and activity (SQSTM1/P62 degradation and LC3-II levels in the presence of lysosomal inhibitors) and fusion (shown using an RFP-GFP-LC3 reporter). To determine the role of the enhanced autophagy we applied either pharmacological autophagy inhibitors (3-methyladenine or pepstatinA/E64) or lentiviral vectors delivering shRNAs targeting *Beclin1* or *Atg7*. Both strategies reduced KaHx-induced neuronal death. A pro-death role of autophagy was also confirmed by the enhanced toxicity of KaHx in cultures overexpressing BECLIN1 or ATG7. Finally, *in vivo* inhibition of autophagy by intrastriatal injection of a lentiviral vector expressing a *Beclin1*-targeting shRNA increased the volume of intact striatum in a rat model of severe neonatal cerebral HI. These results clearly show a death-mediating role of autophagy in hypoxic-excitotoxic conditions and suggest that inhibition of autophagy should be considered as a neuroprotective strategy in HI brain injuries.

Introduction

Macroautophagy, the main type of autophagy (hereafter called simply autophagy), consists of the engulfment of part of the cytoplasm in a multimembrane compartment (autophagosome), which then fuses with a lysosome to produce a large secondary lysosome (autolysosome).[1] Autophagy is essential to the long term health of cells (including neurons) and by preserving cellular homeostasis and supplying nutrients, an increase in autophagy can contribute to cell survival in some stress conditions such as nutrient and growth factor deprivation or accumulation of toxic molecules (pathogens, misfolded proteins, damaged organelles). However, in other situations, autophagy can be deleterious and contribute to cell death either by triggering apoptosis or necrosis or as an independent cell death mechanism ("autophagic cell death" or type II programmed cell death). [2,3] In neurons the question of whether enhanced autophagy promotes cell death or cell survival is a subject of considerable debate[3-8] especially in excitotoxic conditions such as cerebral ischemia. Some studies have suggested a protective role of neuronal autophagy in cerebral hypoxia/ischemia (HI)[9,10] whereas others have demonstrated a death-mediating role [11-14]. In the standard model of cerebral HI in rodent pups,[15] which is widely used for investigating the neuropathological processes of perinatal asphyxia, autophagy is greatly increased in dying cortical and hippocampal neurons [11,16], but the role of this autophagy in neonatal HI brain injury is unclear. Whereas experiments involving pharmacological modulation of autophagy have suggested a protective role,[9] neuron-specific deletion of the autophagy gene (atg) *Atg7* has provided evidence for a deleterious effect.[11]

The present study aims to clarify the role of enhanced neuronal autophagy in HI-induced injury. Excitotoxicity, a pathological process involving the overstimulation of excitatory neurotransmitter receptors (mainly to glutamate), and hypoxia/reoxygenation-induced detrimental pathways are considered as central players in neuronal death after HI. Our aim was to develop an

in vitro model involving doses of an excitotoxin and hypoxia that were toxic in combination but not when used separately so as to imitate as closely as possible the situation in hypoxic-ischemic brain damage. For the reasons explained above and in Results, we selected as excitotoxin kainate (Ka), a potent glutamate receptor agonist that targets non-NMDA glutamate receptors. Furthermore, Ka induces both excitotoxicity[17,18] and autophagy *in vitro*[19] and *in vivo.*[18,20] Ka treatment was applied in a hypoxic environment since hypoxia can exacerbate the mitochondrial production of reactive oxygen species (ROS), especially H_2O_2 and O_2-, which can regulate autophagy[21-25] or inversely autophagy can contribute to oxidative stress by its involvement in ROS accumulation.[26,27] We here show that the combination of Ka and hypoxia (KaHx) activates autophagy and that this mediates neuronal death as demonstrated by the protective effects of downregulating two important Atg proteins, BECLIN1 (BECN1) and ATG7, and by the sensitization to KaHx when both proteins are upregulated. Importantly, the downregulation of BECN1 in a rat model of neonatal HI affords neuroprotection. Taken together these results provide strong evidence for a death-mediating role of enhanced autophagy in HI neuronal injury.

Results

Kainate/hypoxia treatment induces excitotoxic neuronal death

In order to develop an *in vitro* model of cerebral asphyxia, we subjected cultured neurons to hypoxia and excitotoxicity since these are known to be the main mediators of hypoxic-ischemic neuronal death. In initial experiments with NMDA as excitotoxin, we failed to find a dose that was toxic in combination with hypoxia but not in isolation (see Introduction), but further experiments with Ka fulfilled this criterion. Thus, primary cortical neurons were subjected to both 30 μM kainate (Ka) and hypoxia (Hx) at 6% of oxygen for 30 min. Whereas the separate treatments with Ka or Hx were found not to be neurotoxic, their combination was highly effective in promoting neuronal cell death as shown by a strong increase in PI-positive nuclei at 3h and 6h after KaHx treatment (**Fig. 1**).

To characterize further this KaHx-induced neuronal death, we pre-treated cortical neuronal cultures with either EGTA (a chelator of extracellular calcium) (5 mM) or the NMDA receptor antagonist MK801 (40 μM). Both pre-treatments were strongly neuroprotective against KaHx treatment (**Fig. S1A**). These results demonstrate that the KaHx-induced neuronal death is calcium-dependent and mediated by NMDA receptors, even though Ka does not directly activate NMDA receptors.

Inhibition of apoptosis did not prevent kainate/hypoxia-induced neuronal death

We investigated whether KaHx treatment induced apoptosis, using also the classical apoptotic stimulus, staurosporine (STS) (1μM),[28] as a positive control. KaHx-induced neuronal death, unlike that induced by STS, appeared to be caspase-independent. This was suggested by a very weak activation of caspase-3 (**Fig. S2A**) and was confirmed by the fact that apoptosis inhibition - either by overexpression of the anti-apoptotic protein BCL2 or by treatment with the pan-caspase

inhibitor Q-VD-OPH- failed to protect neurons against KaHx. Overexpression of BCL2 (**Fig. S2B**), which was very efficient in preventing STS-induced CASPASE-3 (CASP3) activation (**Fig. S2C**), and eliminated the weak KaHx-induced CASP3 activation that was induced by KaHx (**Fig. S2D**), was unable to protect cortical cultured neurons against KaHx-induced cell death (**Fig. S2E**). A similar lack of protection was observed when KaHx-treated neurons were pre-treated with the pan-caspase inhibitor Q-VD-OPH (25 µM) (**Fig. S2F**).

Kainate/hypoxia treatment enhances neuronal autophagy

To investigate whether autophagy could be involved in KaHx-induced neuronal death, the effect of KaHx treatment on autophagosome formation was studied. As shown in Figure 2A, KaHx-treated neurons showed more autophagosomes compared to control conditions as demonstrated by an increase both in LC3-II expression by immunoblot (**Fig. 2A**) and in the number of LC3-positive dots per neuron revealed by immunocytochemistry and confocal microscopy (**Fig. 2B**) at 3h and 6h following KaHx treatment. Furthermore, we also showed that this KaHx-induced autophagosome accumulation is dependent on NMDA receptor stimulation and extracellular Ca^{2+} since pre-treatment with either MK801 or EGTA were able to prevent the LC3-II increase induced by KaHx treatment (**Suppl. Fig. 1B**). Individual treatments with Ka or Hx did not result in any significant change in LC3-II expression (**Suppl. Fig. S3**).

The effect of KaHx on lysosomes was then evaluated using immunocytochemistry against LAMP1 (Lysosomal Associated Membrane Protein 1) (**Fig. 2C**) and CATHEPSIN B (CTS B) (**Fig. 2D**). KaHx induced not only an increase in the number of both LAMP1- (**Fig. 2C**, left histogram) and CTS B-positive (Fig. 2D, left histogram) dots, but also an increase in the size of both LAMP1- (**Fig. 2C**, right histogram) and CTS B-positive dots (**Fig. 2D**, right histogram) as

shown by a rise in the number and the percentage of the largest dots (>0.5µm^2) which are presumably autolysosomes produced by fusion between autophagosomes and lysosomes.

Finally, to demonstrate definitively that KaHx induced an increase in the autophagic flux, additional experiments were conducted. First, decreased expression of SQSTM1/P62, a long-lived protein preferentially degraded by autophagy, was shown at 3 h and 6 h after KaHx treatment as shown by immunoblot (**Fig. 3A**). Moreover, treatments with Ka or Hx alone did not result in any significant change in SQSTM1/P62 expression (**Suppl. Fig. S3A**), which is as expected since these separate treatments did not enhance autophagy. To check that the decrease in SQSTM1/P62 expression after KaHx was not due to an effect on its production, we did additional experiments using a dose of 1µg/µl cycloheximide (CHX), which prevents more than 95% of the protein synthesis. CHX treatment for 6 h significantly decreased SQSTM1 expression as expected. But, importantly, in the presence of CHX the stimulus KaHx (6 h) still induced a significant decrease in SQSTM1 expression, supporting the KaHx-induced enhancement of autophagic flux (**Suppl. Fig. S3B**). Then, cortical neurons were pre-treated with a combination of the lysosomal enzyme inhibitors E64 (10 µg/ml) and pepstatin A1 (PepA) (10 µg/ml). The KaHx-induced accumulation of LC3-II was greater in E64/PepA-treated cultures than in untreated cultures (**Fig. 3B**), showing that KaHx treatment induced the neoformation of autophagosomes. To further confirm an increase in the autophagic flux induced by KaHx and to demonstrate that KaHx did not impair the autophagosome/lysosome fusion process, autophagic flux was monitored with the tandem mRFP-GFP-LC3–expressing plasmid ptfLC3 (**Fig. 3C and D**) [29]. KaHx induced an increase in both the number of early autophagosomes (yellow dots, before fusion) and late autophagosomes (red dot, after fusion with the lysosome) per neuron after both 3h and 6h of KaHx treatment.

Taken together, these results clearly demonstrate that KaHx treatment induced an enhancement of the autophagic flux.

Autophagy contributes to kainate/hypoxia-induced neuronal death

Having demonstrated that autophagy is induced by KaHx treatment, the next step was to evaluate the functional role of this enhanced autophagy in KaHx-induced cell death. First, the effect of pharmacological inhibition of autophagy with 3-methyladenine (3-MA) was tested. As expected, pre-treatment with 3-MA (10 mM) prevented the increases in both LC3-II expression and SQSTM1/P62 degradation (**Fig. 4A**). Then 3-MA treatment displayed a significant neuroprotective effect as demonstrated by a decrease in PI-positive nuclei 6h after KaHx treatment (**Fig. 4B**). We also evaluated the effect of lysosomal enzyme inhibition on KaHx-induced neuronal death by using combined treatment with the above-mentioned cocktail of E64 and PepA. Pre-treatment with E64/PepA, that efficiently blocked autophagic degradation (**Fig. 3B**), significantly reduced neuronal death induced by KaHx (**Fig. 4C**).

To confirm this death-promoting role of enhanced autophagy in KaHx-induced neuronal death, we performed knock-down of two different autophagy genes (*Atg7* and *Becn1*) using lentiviral vectors encoding short hairpin RNAs (shRNAs). Transduction of cultured cortical neurons with *Atg7*- and *Becn1*-targeting shRNA vectors resulted in large reductions in the levels of the corresponding proteins (**Fig. 5A** and **B**). As expected, downregulation of both ATG7 and BECN1 decreased KaHx-induced autophagy as shown by both a decrease in autophagosome formation (47% and 57% reduction in LC3-II for shRNAs targeting *Atg7* and *Becn1* respectively) and the inhibition of SQSTM1/P62 degradation (**Fig. 5C** and **D**). Quantification of PI-positive nuclei or of lactate dehydrogenase release 6h after KaHx treatment demonstrated a significantly reduced toxicity in *Atg7* shRNA and *Becn1* shRNA transduced neurons, confirming a pro-death

role of autophagy following KaHx treatment (**Fig. 5E** and **F, Suppl. Fig. S4A**). This neuroprotective effect was still observed at 24h after KaHx treatment (**Suppl. Fig. S4A** and **S4B**).

To corroborate these results, we overexpressed BECN1 and ATG7 in cortical neuronal cultures using lentiviral vectors encoding ATG7-myc and BECN1-myc. Expecting that KaHx-induced neuronal death would occur more rapidly when ATG7 and BECN1 were overexpressed, we chose an earlier time-point (3h) point for the overexpression experiments. Overexpression of either BECN1 or ATG7 (**Fig. 6A** and **B**) resulted in an increased autophagic response to KaHx as shown by significantly higher expression of LC3-II and reduced expression of SQSTM1/P62 (**Fig. 6C** and **D**). Furthermore, overexpression of ATG7 or BECN1 exacerbated KaHx-induced neuronal death, as shown by increased numbers of PI-positive neurons 3h after KaHx treatment in both cases (**Fig. 6E** and **F**).

Since apoptosis and autophagy share common regulators we investigated the effect of apoptosis inhibition on KaHx-induced autophagy. Neither BCL2 overexpression using lentiviral vectors (**Fig. S2**) nor caspase inhibition using Q-VD-OPH (data not shown) had any effect on KaHx-induced autophagy.

Autophagy is increased and involved in neonatal cerebral hypoxic-ischemic brain injury

The functional role of autophagy in *in vivo* pathological situations involving hypoxic-excitotoxic brain injuries was then investigated. We had previously shown that neonatal cerebral hypoxia-ischemia (HI) enhanced neuronal autophagy in the cortex and the CA3 region of the hippocampus [16], and we here show that a similar enhancement of autophagy occurred in the striatum in the same HI model. We selected the striatum rather than the cortex for the *in vivo* experiments because the striatum's spheroidal form and limited extent permitted us to knock

down genes throughout the entire structure using lentiviral vectors (**Suppl. Fig. S5)**. Autophagy is enhanced at 24h after the insult by an increase in LC3-II level (**Fig. 7A**), and by an increase in the number of autophagosomes in striatal neurons double-immunolabeled with the neuronal marker NeuN and LC3 (**Fig. 7B**). Moreover, immunoblots revealed that neonatal HI decreased the striatal levels of SQSTM1/P62 expression, also at 24h after HI (**Fig. 7C**). Histochemistry for β-hexasosaminidase, a lysosomal enzyme, revealed a strong increase of β-hexasosaminidase-positive dots detected at 24h after HI compared to sham animals (**Fig. 7D**). Taken together, these results showed that autophagy is strongly increased in the striatum after neonatal cerebral HI.

The role of this enhanced autophagy in striatum after neonatal cerebral HI was investigated by downregulation of BECN1 by intra-striatal injection of lentiviral vectors expressing *Becn1* shRNA, which decreased BECN1 expression by 30% (**Fig. 8A**). At 24h after HI, BECN1 knock-down reduced the HI-induced LC3-II increase and SQSTM1 degradation (**Fig. 8B**), and increased the percentage of striatal intact tissue (**Fig. 8C**). Thus, our *in vivo* results provide evidence for a death-mediating role of autophagy in neonatal cerebral HI.

Discussion

It is now generally recognized that autophagic processes are activated in excitotoxic conditions, and notably cerebral ischemia. Increased numbers of autophagosomes have been described in different *in vitro* situations of excitotoxicity such as long treatment and/or high doses of NMDA[30,31] or Ka,[19] or exposure to a specific glutamate uptake inhibitor.[32] The injection of toxic doses of Ka into the adult mice hippocampus[20,33] or striatum[34,35] also induces autophagy. Numerous *in vivo* studies of cerebral ischemia or HI over the past twenty years have likewise shown enhanced neuronal autophagy (autophagosome formation and lysosomal activity).[13,14,36-42] Controversies remain, however, concerning the role of the autophagic activation in excitotoxic conditions both *in vitro* and *in vivo*. Even though most of the papers demonstrate a pro-death function of autophagy,[11-14,27,31,33,34,37,43,44] some studies suggest the opposite.[9,10,45-49] These discrepancies could be due to differences in the excitotoxic conditions, to the use of pharmacological inhibitors with limited specificity[50,51] or to the lack of complete analysis on autophagy flux, i.e. demonstration that autophagosome increase is not due to lysosomal dysfunction in excitotoxic situations. We here resolve these problems and provide clear evidence that neuronal autophagy in hypoxic-excitotoxic conditions is deleterious.

The combination of two stimuli, a low dose of Ka and moderate hypoxia (6% O_2), each of which are nontoxic when applied for a very short period (30min), produces a powerful and synergetic excitotoxic stimulus. By comparison with the in vivo situation, 6% O_2 is in fact normoxic, not hypoxic, but when neurons cultured in standard conditions (at 21% O_2) are exposed to 6% O_2 this constitutes a hypoxic stress, probably because they have reduced mitochondrial function compared with ones cultured at 5% or 2% O_2.[52] It has been shown that Ka is more potent than NMDA in release of endogenous glutamate.[53] Moreover different studies support the essential role of KA receptors (Gluk2, Gluk4) in excitotoxicity both *in vitro* and *in*

vivo, partially involving MAPK activation.[54,55] Interestingly, in the rat model of neonatal HI used in this study, neither the systemic hypoxia nor the common carotid occlusion alone produces brain damage, whereas the combination of both causes a very severe lesion.[15] Ka and hypoxia can mutually exacerbate their negative effects.[56,57] A study in a guinea pig model of perinatal hypoxia has shown that hypoxia can decrease the affinity and change the kinetic of desensitization of Ka receptors suggesting a potential role of Ka receptors in hypoxia-induced excitotoxicity.[58] Interestingly, in humans a transient developmental elevation in KA binding in early life could correlate with the period of vulnerability of this cerebral region to hypoxia-ischemia.[59]

We clearly demonstrated in this study that KaHx enhanced autophagic flux. The number of autophagosomes (LC3-positive dots, LC3-II expression level) was increased along with an activation of lysosomal activity (shown by degradation of SQSTM1/P62, increase in the number and size of lysosomes labeled with LAMP1 or CTS B antibodies) and an increase in autophagosome-lysosome fusion (shown with an mRFP-GFP-LC3–expressing plasmid). Prevention of this KaHx-induced autophagy, not only pharmacologically with 3-MA but also more specifically by downregulating ATG7 or BECN1, significantly decreased neuronal death. Moreover upregulation of either protein, which activated autophagy, aggravated the neuronal death. These results strongly suggest that enhanced autophagy is involved in KaHx-induced cell death.

In vivo experiments have shown that intrastriatal injection of Ka in adult rats induced an excitotoxic injury that was decreased by both pre- and post-treatments with 3-MA.[34] More recently, both 3-MA injection and ATG7 downregulation have been shown to reduce the loss of hippocampal neurons provoked by intraperitoneal administration of Ka.[33] Both studies imply that autophagy can contribute to Ka-induced apoptosis. However in the present *in vitro* model, KaHx triggers a very rapid and strong neuronal death, with no apparent involvement of apoptosis since

neither the pan-caspase inhibitor Q-VD-OPH nor BCL2 overexpression have a protective effect. The involvement of caspases is known to vary between excitotoxicity models.[60, 61] It has also been shown that 3-MA can suppress the mitochondrial ROS production associated with Ka-induced excitotoxicity in cultured striatal neurons[19]. Enhanced autophagy may therefore contribute to oxidative stress induced by KaHx. We showed also a protective effect of inhibiting lysosomal activity with E64/PepA suggesting that autophagic degradation is involved as well in neuronal death. Removal of some protective proteins such as antioxidants[26] or generation of toxic molecules like ferric iron[62] may be implicated. Autophagosomes and (auto)lysosomes have also been shown to be potential ROS sources.[27]

There is controversy about the role of the autophagy in neonatal HI. Induction of autophagy with the pharmacological agent rapamycin provided some protective effects against cerebral HI in rat pups when injected before hypoxia.[9] On the other hand, the work of Koike et al. (2008)[11] demonstrated that ATG7 deficiency specifically in neurons affords strong neuroprotection against HI-injury in the hippocampus of neonatal mice. Our results support the latter study by showing both *in vitro,* and for the first time *in vivo,* that autophagy inhibition by knockdown of autophagy genes is neuroprotective. This was the first time that downregulation of BECN1 was achieved *in vivo* requiring the use of lentiviral vectors. This downregulation decreased the stress-induced autophagy and reduced the striatal damage induced by HI in rat pups. We also previously demonstrated that post-treatment with 3-MA during the 4.5 hours following the onset of ischemia decreased by half the volume of the cortical lesion in a model of middle cerebral artery occlusion in rat pups.[12,43] Most – though not all[47,48] - studies of adult cerebral ischemia likewise suggest a death-mediating role of autophagy when it is inhibited with 3-MA,[13,27,37] with lysosomal inhibitors[13,27,63] or with BECN1 knockdown.[14]

These results help open the way to possible therapy against neonatal HI by inhibition of autophagy, but this would need to be by transient inhibition, since constitutive autophagy is required for neuronal health and even survival.[64, 65]

In conclusion our study gives a clear demonstration of the pro-death role played by induced autophagy in excitotoxic-hypoxic conditions in cultured neurons and neonatal rats, and it consolidates the idea that strategies targeting excessively activated autophagy, to inhibit it transiently, should be considered in the development of new therapeutic approaches against hypoxic-ischemic brain injuries.

Materials and Methods

Primary cortical neuronal culture. Sprague-Dawley rat pups (from Janvier, France) were euthanized in accordance with the Swiss Laws for the protection of animals and were approved by the Vaud Cantonal Veterinary Office. Primary neuronal cultures from cortices of 2-day-old rats were prepared and maintained at 37°C with a 5% CO_2-containing atmosphere in neurobasal medium (Life Technologies, 21103-049) supplemented with 2% B27 (Invitrogen, 17504044), 0.5 mM glutamine (Sigma, G7513) and 100 µg/ml penicillin-streptomycin (Invitrogen) as described previously.[66] Western blot analyses were done on neurons plated at a density of ~$7x10^5$ cells/dish (35 mm poly-D-lysine precoated dishes, BD Biosciences, 356467) and immunocytochemistry on neurons plated at a density of ~$3x10^5$ cells on 12 mm glass coverslips coated with 0.01% poly-L-lysine (Sigma, P4832). Experiments were performed at 12-13 days in vitro (DIV). These cultures contain around 10-15% of non-neuronal cells (MAP2 or NeuN-negative). The n values in the different results refer to the number of independent experiments, each involving 2 or 3 culture dishes or coverslips. Thus, the mean value of 2-3 dishes or coverslips was counted as a single observation.

Rat model of perinatal asphyxia. All experiments were performed in accordance with the Swiss Laws for the protection of animals and were approved by the Vaud Cantonal Veterinary Office. Seven-day old male rats (Sprague Dawley, from Janvier, France) underwent hypoxia-ischemia (HI) according to the Rice-Vannucci model[15] adapted from the Levine procedure[67] as described previously.[68] Briefly, under isoflurane (3%) anaesthesia, the right common carotid artery was isolated, double-ligated (Silkam, 5/0, B/BRAUN Aesculap) and cut. After 2h of recovery with the dam, the rat pups were exposed to 2h of systemic hypoxia at 8% of oxygen in a humidified

chamber maintained at 35.5°C. Sham operated animals (same anesthetic and surgical procedures but without section of the common carotid artery) were used as controls.

Kainate-hypoxia (KaHx) stimulation. Hypoxia was performed for 30 min. in a sealed modular incubator chamber (Billups-Rothenberg, MIC-101) that had been flushed for 5 min with a gas mixture at 6% of oxygen. At the start of the 30 min. of hypoxia, all the (neurobasal) culture medium was replaced with bicarbonate-buffered saline (BBS) solution (NaCl 116mM, KCl 5.4mM, $MgSO_4$ 0.8mM, NaH_2PO_4 1mM, $NaHCO_3$ 26.2mM, Glycine 0.01mM, $CaCl_2$ 1.8mM, 4.5 mg/mL glucose (reagents from Sigma-Aldrich)) previously deoxygenated for 1h30 in the hypoxic chamber. Kainate (30 µM) was added immediately after the BBS, and the neuronal cultures were thus exposed to KaHx stimulation during the 30min of hypoxia. Then, the BBS was removed and replaced with the previous neurobasal medium that had been reserved mixed with one-third volume of fresh medium. Thirty minutes in normoxic BBS was used as the control stimulation (ct).

Pharmacological treatments. Primary cortical neuronal cultures were pre-treated for 1h with 25 µM Q-VD-OPH (Quinoline-Val-Asp(ome)-Ch2-O-phenoxy; MP Biomedicals, 030PH10903), 10 mM 3-methyladenine (3-MA) (Sigma-Aldrich, M9281), 5 mM EGTA (Sigma-Aldrich, E0396) or 40 µM MK801 (Sigma-Aldrich, M107). For inhibition of lysosomal degradation, a cocktail of 10 µg/ml Pepstatin A1 (PepA) (Sigma-Aldrich, P5318) and 10 µg/ml E64 (Sigma-Aldrich, E3132) was applied for 6h prior to KaHx stimulation.

Immunoblotting. Cortical neurons or striatal brain tissue were collected in lysis buffer (20 mmol/L HEPES, pH 7.4, 10 mmol/L NaCl, 3 mmol/L $MgCl_2$, 2.5 mmol/L EGTA,

0.1 mmol/L dithiothreitol, 50 mmol/L NaF, 1 mmol/L Na_3VO_4, 1% Triton X-100 (reagents from Sigma-Aldrich), and a protease inhibitor cocktail (Roche)). Proteins were separated by SDS-PAGE, transferred on nitrocellulose membrane and analyzed by immunoblotting. Antibodies were diluted in a blocking solution containing 0.1% casein and 0.1% Tween 20. The following primary antibodies were used for protein immunodetection: anti-α-tubulin (sc-8035) mouse monoclonal, anti-ATG7 (sc-33211) rabbit polyclonal and anti-BECN1 (sc-11427) rabbit polyclonal from Santa Cruz Biotechnology (Santa Cruz); anti-LC3 (NB100-2220) rabbit polyclonal from Novus Biologicals; anti-cleaved caspase-3 (9661) rabbit polyclonal and anti-BCL2 (2870) rabbit monoclonal from Cell Signalling Technology; anti-SQSTM1 (P0067) rabbit polyclonal from Sigma-Aldrich. After washes in PBS-0.1% Tween, polyclonal goat anti-mouse or anti-rabbit IgG secondary antibodies were applied (IRDye 680 (LI-COR, B70920-02) or IRDye 800 (LI-COR, 926-32210)). The Odyssey Infrared Imaging System (LI-COR) was used to analyze protein bands using Odyssey v1.2 software (LI-COR). OD values were normalized against tubulin and expressed as a percentage of values obtained with neurons after control stimulation (100%).

Lentiviral vectors. Downregulations of Atg were performed with pLKO lentiviral vectors (Openbiosystems) expressing rat specific shRNA sequences from TRC (the RNAi consortium) library as described previously:[28] a combination of TRCN0000092163 and TRCN0000092166 for ATG7 (GenBankTM NM_001012097) and TRCN0000033552 for BECN1 (GenBankTM NM_053739.2). ATG7 and BECN1 overexpressions were achieved by self-inactivating lentiviral transfer vectors under the control of mouse phosphoglycerate kinase 1 (PGK) promoter (SIN-W-PGK) transducing cDNAs sequences encoding full-length rat *Atg7* (GenBankTM

NM_001012097) and *Becn1* (GenBankTM NM_053739) created using PCR with specific primers (*Atg7*: nucleotides 16-35 (forward), 2092-2112 (reverse); *Becn1*: nucleotides 225-243 (forward), 1549-1570 (reverse)) to which the myc-tag encoding sequence was added as explained previously.[28] Primary cortical neuron cultures were infected at DIV7 with 50ng p24/ml culture medium for each vector, and half the medium was replaced on DIV11. A pLKO vector containing scrambled shRNA (Openbiosystems) in Atg knockdown experiments or a SIN-W-PGK empty vector in ATG upregulation experiments were used as control vectors.

mRFP-GFP-LC3 plasmid transfection and quantification. This plasmid permits the distinction between acidic and non-acidic LC3-positive structures, because GFP is acid-sensitive whereas RFP is not. Neurons on coverslips were transfected using Lipofectamine 2000 (Invitrogen, 11668-019) as described previously.[69] In brief, two thirds of the medium was removed and replaced for 5 h by fresh Neurobasal medium (Life Technologies, 21103-049) plus transfection mix with the tandem mRFP-GFP-LC3–expressing plasmid ptfLC3 (Addgene) (1µg of DNA for 6µl of Lipofectamine). Confocal images were acquired using a Zeiss LSM 710 Meta confocal laser scanning microscope. Total LC3-positive dots (GFP+ RFP+ and GFP- RFP+ dots), early autophagosomes (GFP+ RFP+ dots) and late autophagosomes (GFP- RFP+ dots) were analyzed using ImageJ software and expressed as a number of positive dots per neuron per μm^2.

Quantification of cell death with propidium iodide. Cortical neurons on coverslips were washed in PBS 1 mM $MgCl_2$ at 4°C and incubated for 10 min in propidium iodide (PI, Sigma-Aldrich, P4170) diluted in PBS $MgCl_2$. After PBS washes neurons were fixed in 4% paraformaldehyde in 0.1M PBS (pH 7.4) for 15 min. A Hoechst staining was performed to visualize the total number of nuclei. Coverslips were mounted with FluorSave (Calbiochem, 345-789-20). Cells were

examined using a Zeiss Axioplan 2 imaging microscope. Results were expressed as a percentage of PI-positive nuclei relative to Hoechst-positive nuclei.

Lactate dehydrogenase release. Cell death was assayed by measurement of lactate dehydrogenase released in the medium using the Cytotox 96 non-radioactive cytotoxicity assay kit (Promega, G1780) as previously described.[66] Lactate dehydrogenase measurements were normalized with respect to the values with control vector 6h after KaHx treatment condition.

Intrastriatal injection of lentivirus. Lentiviral vectors were stereotaxically injected in the right striatum of 1 or 2-day old rat pups (**Suppl. Fig. S5)**. Rats were anesthetized with isoflurane (3%) and positioned in a stereotaxic frame. A midline scalp incision and a small hole were made in the skull. A 5.0 µl Hamilton syringe was used for injection at a site specified by the following stereotaxic coordinates from Bregma: 0.5 mm anterior, 2.5 mm right and 3 mm depth from the skull surface. One µl of lentiviral suspension was infused over 5 min with an automatic injector. The needle stayed in place for 2min before a slow removal. Lentiviral suspensions were prepared by mixing SIN-W-PGK vector encoding YFP (to visualize the infected area) and pLKO vectors encoding control or BECLIN1 shRNA at 1:1 ratio and with a particle content normalized to 125000 µg p24/ml for each lentivirus. For immunoblotting studies infected striatal tissue was dissected under a stereomicroscope with fluorescence (Leica MZ16FA).

Measurement of the surviving striatum after neonatal hypoxia-ischemia. The lesion volumes were measured 24h after the insult. Perfused and frozen brains were entirely cut into 50 µm coronal sections disposed in series. In a series of cresyl violet stained sections spaced at 500 µm, the contralateral striatum and the intact ipsilateral striatum areas were measured using the

Neurolucida program (MicroBrightField) and the corresponding volumes were then calculated with Neuroexplorer (MicroBrightField). The surviving striatum was then expressed as a percentage of contralateral striatum volume.

Immunostaining. Immunostainings were performed on primary cortical neurons that had been cultured on coverslips and fixed with 4% paraformaldehyde for 15min, and on 18µm cryostat brain sections from rat pups that had been perfused intracardially with the same fixative. Blocking and permeabilization were done in PBS with 15% donkey serum and 0.3% Triton X-100 for 30-45 min. Primary antibodies were diluted in PBS with 1,5% donkey serum and 0.1% Triton X-100 overnight at 4°C. Secondary antibodies were diluted in PBS for 2h at room temperature.

The following primary antibodies were used: anti-cathepsin B (06-480) rabbit polyclonal antibody from Upstate Biotechnology; anti-NeuN (MAB377) mouse monoclonal antibody and anti-MAP2 rabbit (AB5622) from Chemicon; anti-LAMP1 (428017, for rat) from Calbiochem. Anti-LC3 was a generous gift from Prof. Yasuo Uchiyama (Tokyo, Japan).

For immunofluorescence labelling, Alexa Fluor 488 or 594 donkey-anti-rabbit or mouse secondary antibodies (Invitrogen) were used and sections or coverslips were mounted with FluorSave after a Hoechst staining. A LSM 510 Meta confocal microscope (Carl Zeiss) was used for confocal laser microscopy. Images were processed with LSM 510 software and mounted using Adobe Photoshop.

For immunoperoxidase labelling on rat brain sections, endogenous peroxidases were quenched in 0.3% H_2O_2 in methanol for 20min before incubation in blocking medium. After the incubation in biotinylated secondary antibody (Jackson Immunoresearch), avidin- biotinylated peroxidase complex (VECTASTAIN Elite ABC Kit Vector, PK-6200) was added for 2h at room temperature

and then developed by incubation with diaminobenzidene (DAB, Roche, 11718096001) substrate solution. The sections were dehydrated in graded alcohols and mounted in Eukitt. Sections were analyzed using a Zeiss Axioplan 2 imaging microscope.

N-Acetylhexosaminidase histochemistry. Experiments were performed as described previously.[12] Briefly, sections were incubated for 1 hour at 37°C in Fast red violet salt solution (0.63 mol/L ethylene glycol monomethyl ether, 1% polyvinyl pyrrolidone, 0.1 mol/L citric acid-citrate buffer (pH4.4), 1.6 mol/L sodium chloride, 2.7 mmol/L 5-chloro-4-benzamido-2-methylbenzene-diazonium chloride (Fast red violet LB salt) (Sigma-Aldrich, F3381) using 0.5 mmol/L naphthol-AS-BI-*N*-acetyl-D-glucosaminide (Sigma-Aldrich, N4006) as the substrate. The sections were then fixed in 10% formaldehyde, dehydrated in graded alcohols and mounted in Eukitt medium. To verify the staining specificity, controls with omission of the substrate or at basic pH (pH 10) were done in parallel. Image acquisition was performed with an Axiovision Zeiss microscope.

Statistical analysis. Data are expressed as mean values ± SEM. Data were analyzed statistically using JB STAT software. The n values were sufficiently high for the statistical power to be greater than 0.8 in all experiments. We first tested each group of data for distribution normality using Shapiro-Wilk tests. In case of normal distribution, we used a Welch's ANOVA test (one-way ANOVA with unequal variances) followed by a post-hoc Tukey-Kramer test to compare the different treatments. When the distribution was not normal, we used a Kruskal-Wallis test (non-parametric analogue of the one-way ANOVA) followed by a post-hoc Steel-Dwass test to compare the different treatments. $p < 0.05$ was chosen as the threshold for statistical significance.

Figure Legends

Figure 1. Kainate/hypoxia treatment induces neuronal death.

(A) KaHx induces neuronal death as shown morphologically in brightfield images or by combined propidium iodide (PI)-staining (in red, dead cells) and MAP2-immunolabeling (in green) 6 h after control and KaHx stimulations. **(B)** Representative images of PI-stained (in red) and Hoechst-stained nuclei (in blue, total cells) of cultured cortical neurons 6 h following 30 min of different stimulations: ct: control, KaHx: kainate/hypoxia, Ka: kainate, Hx: hypoxia. **(C)** Quantification of PI-positive nuclei as a percentage of all nuclei showing a rapid and strong cell death induced by the combination of kainate and hypoxia whereas the separate treatments were not toxic (ct: 5 ± 2%, KaHx 3 h: 44 ± 6%, KaHx 6 h: 59 ± 3%, Ka: 11 ± 2%, Hx 6 ± 2%). Values are mean ± SEM, *p < 0.05, ***p< 0.001, Tukey-Kramer test. n = 6 independent experiments. Bar = 20 µm.

Figure 2. Kainate/hypoxia increases autophagosome formation and lysosomal markers in cultured cortical neurons.

(A) Representative immunoblot of LC3 (upper part) and the corresponding quantification (lower part) showing that LC3-II expression level is upregulated at 3 h and 6 h after kainate/hypoxia (KaHx) stimulation. (ct: 100 ± 0%, KaHx 3 h: 160 ± 8%, KaHx 6 h: 185 ± 19%). Values are mean ± SEM, ***p< 0.001, Steel-Dwass test. **(B)** Confocal images of LC3 immunolabeling (in red) of representative cultured cortical neurons at 6h after control (ct) or KaHx stimulation (upper part), and quantification of LC3-positive dots per neuron per μm^2 (lower part) demonstrating a strong increase in the number of autophagosomes after KaHx. (ct: 0.028 ± 0.004, KaHx 3 h: 0.189 ± 0.022, KaHx 6 h: 0.224 ± 0.024). Values are mean ± SEM, Tukey-Kramer test. Bar=20

µm. **(C)** Immunolabeling for the lysosomal marker LAMP1 (in green) shows an increase not only in the number of positive dots (upper graph; ct: 0.099 ± 0.006, KaHx 3 h: 0.196 ± 0.009, KaHx 6 h: 0.210 ± 0.017; Tukey-Kramer test) but also in the percentage of large positive dots (>0.5 μm^2) (lower graph; ct: 3.3 ± 1.5%, KaHx 3 h: 23.9 ± 3%, KaHx 6 h: 20 ± 4.8%; Steel-Dwass test) after KaHx. Values are mean ± SEM. **(D)** Similar results are obtained with immunolabeling for the lysosomal enzyme cathepsin B (CTS B) (in red). This phenomenon occurs in neurons as shown by double immunolabeling for CTS B and NeuN (in green). (Upper graph: ct: 0.06 ± 0.01, 3 h KaHx: 0.176 ± 0.02, 6 h KaHx: 0.19 ± 0.02) (Lower graph: ct: 3.4 ± 1.2%, 3 h KaHx: 16.1 ± 1.2%, 6 h KaHx: 16.9 ± 1.7). Values are mean ± SEM, Steel-Dwass test. n≥25. Bar=20µm. *p< 0.05, **p< 0.01, ***p< 0.001. n = 4 independent experiments.

Figure 3. Kainate/hypoxia enhances autophagic flux in cultured cortical neurons.

(A) Representative immunoblots for SQSTM1/P62 (upper part) and the corresponding quantification (lower part) indicate that kainate/hypoxia (KaHx) significantly decreases SQSTM1/P62 expression. (ct: 100 ± 0%, 3 h KaHx: 76 ± 4%, 6 h KaHx: 73 ± 5%). n = 13 independent experiments. **(B)** Representative immunoblots against LC3 and SQSTM1/P62 and the corresponding quantifications demonstrate that exposure to pepstatin A (PepA) and E64 in cultured neurons increases the level of LC3-II (Pep/E64: 174 ± 13%) and SQSTM1/P62 (Pep/E64: 144 ± 14 %) relative to control (ct) stimulation, indicating that autophagic degradation is prevented. Addition of Pep/E64 6 h before, during or after KaHx treatment (6 h) results in a greater increase in LC3-II than treatment with KaHx or E64/PepA alone (Ka+Hx: 169 ± 5%, E64/PepA + KaHx: 277 ± 27%) and diminishes the KaHx-induced degradation of SQSTM1/P62 (Ka+Hx: 78 ± 3%, E64/PepA + KaHx: 118 ± 9%) . Values are mean ± SEM, *p<0.05, **p<0.01, ***p< 0.001, Tukey-Kramer test. n = 4 independent experiments. **(C)** Confocal images of

representative cultured cortical neurons transfected with the tandem mRFP-GFP-LC3–expressing plasmid at 3h and 6h after Ka/Hx. **(D)** Quantification of the number of LC3-positive dots per neuron per μm^2 shows an active autophagic flux (TOTAL = GFP+ RFP+ and GFP- RFP+: ct: 0.03 ± 0%, 3 h: 0.17 ± 0.02%, 6 h: 0.23 ± 0.01%, early autophagosomes = GFP+ RFP+: ct: 0.01 ± 0%, 3 h: 0.10 ± 0.02%, 6 h: 0.13 ± 0.01%,; late autophagosomes = GFP- RFP+: ct: 0.02 ± 0%, 3 h: 0.07 ± 0.01%, 6 h: 0.10 ± 0.01 %,). Values are mean ± SEM,. **p<0.01, ***p< 0.001. Tukey-Kramer test. n = 4 independent experiments. Bar=20µm.

Figure 4. Pharmacological inhibition of the autophagic process with 3-methyladenine or E64/PepstatinA protects cultured cortical neurons against kainate/hypoxia treatment.

(A) Representative immunoblots against LC3 and SQSTM1/P62 and the corresponding quantifications confirm that 3-methyladenine (3-MA) prevents accumulation of LC3-II (KaHx: 164 ± 14%, 3-MA KaHx: 95 ± 14; Welch ANOVA, n = 5 independent experiments) and reduction of SQSTM1/P62 (KaHx: 65 ± 8%, 3-MA KaHx: 110 ± 12%; Welch ANOVA, n = 5 independent experiments) following exposure to KaHx. **(B-C)** Quantification of PI-positive nuclei as a percentage of all nuclei (Hoechst-stained) demonstrates that inhibition of the autophagic process with **(B)** 3-MA (ct: 6.6 ± 1.4, 3-MA: 8.4 ± 1.9, KaHx: 54.8 ± 2, 3-MA KaHx: 24.6 ± 4.8, Steel-Dwass test, n = 3 independent experiments) or **(C)** E64/PepstatinA (PepA) (ct: 7.9 ± 0.1, E64/PepA: 12.5 ± 1, KaHx: 60 ± 3.8, E64/PepA KaHx: 26.7 ± 7.4, Tukey-Kramer test, n = 4 independent experiments) is neuroprotective. Values are mean ± SEM, *p<0.05, **p<0.01, ***p< 0.001.

Figure 5. Inhibition of autophagy by downregulation of ATG7 or BECLIN1 protects cultured cortical neurons against kainate/hypoxia treatment.

(A-B) Representative immunoblots and corresponding quantifications showing that lentiviral transduction of shRNAs against **(A)** *Atg7* or **(B)** *Beclin1* (*Becn1*) reduces the expression of ATG7 (53 ± 2%) or BECN1 (43 ± 2%) compared to control vector-transduced neurons. Values are mean ± SEM, ***p< 0.001, Wilcoxon test. n = 4 independent experiments. **(C-D)** Downregulation of ATG7 or BECN1 inhibits autophagy induced 6h after KaHx. **(C)** ATG7 downregulation significantly reduces LC3-II (control vector KaHx: 163 ± 30%, *Atg7* shRNA KaHx: 68 ± 10%, Kruskal-Wallis test, n = 6 independent experiments) as occurs to a lesser extent with **(D)** BECN1 downregulation (control vector KaHx: 205 ± 22%, *Becn1* shRNA KaHx: 140 ± 15%, ANOVA, n = 5 independent experiments). Knockdown of either protein is however enough to completely block SQSTM1/P62 degradation following KaHx (for ATG7: control vector KaHx: 81 ± 2%, *Atg7* shRNA KaHx: 116 ± 12%, n = 5 independent experiments; for BECN1: control vector KaHx: 82 ± 4%, *Becn1* shRNA KaHx: 123 ± 7%, Welch ANOVA, n = 7 independent experiments). Values are mean ± SEM expressed as a percentage of control (ct) stimulated neurons transduced with control vector, **p< 0.01, ***p< 0.001. **(E-F)** Transduced neurons with *Atg7* and *Becn1* shRNAs are less sensitive to KaHx than control vector transduced neurons as demonstrated by a significant decreased number of PI-positive nuclei 6h after the stimulation (for ATG7: control vector: 2 ± 0.7%, *Atg7* shRNA: 5 ± 2%, control vector KaHx: 62 ± 2%, *Atg7* shRNA KaHx: 46 ± 3%; for BECN1: control vector: 2 ± 0.8%, *Becn1* shRNA: 5 ± 1%, control vector KaHx: 59 ± 2%, *Becn1* shRNA KaHx: 30 ± 4%). Values are mean ± SEM expressed as a percentage of all nuclei (Hoechst-stained). **p< 0.01, Steel-Dwass test, n = 8 independent experiments.

Figure 6. Upregulation of autophagy by overexpression of ATG7 and BECLIN1 sensitizes cultured cortical neurons against kainate/hypoxia treatment.

(A-B) Representative immunoblots and corresponding quantifications showing that lentiviral transduction of **(A)** ATG7-myc and **(B)** BECLIN1 (BECN1)-myc strongly increase expression of ATG7 (430 ± 32%) and BECN1 (220 ± 20%) compared with control vector transduced neurons. Values are mean ± SEM, Wilcoxon test. n = 4 independent experiments. **(C)** The very strong overexpression of ATG7 enhances the autophagic process induced 3h after KaHx as demonstrated by an increase in LC3-II (control vector KaHx: 139 ± 3%, ATG7-myc KaHx: 189 ± 15%, Kruskal-Wallis test, n = 6 independent experiments) and by a reduction of SQSTM1/P62 (control vector KaHx: 83 ± 1%, ATG7-myc KaHx: 65 ± 5%, Welch ANOVA, n = 5 independent experiments). **(D)** The two-fold increase in BECN1 expression significantly increases the level of LC3-II (control vector KaHx: 134 ± 2%, BECN1-myc KaHx: 156 ± 7%, Welch ANOVA, n = 4 independent experiments) and decreases the level of SQSTM1/P62 (control vector KaHx: 81 ± 2%, BECN1-myc KaHx: 72 ± 5%, Kruskal-Wallis test, n = 6 independent experiments) 3 h after KaHx. Values for **(C)** and **(D)** are mean ± SEM expressed as a percentage of control (ct) stimulated neurons transduced with control vector. **(E-F)** Neurons transduced with ATG7-myc and BECN1-myc expression vectors are more sensitive to KaHx than control vector-transduced neurons as is demonstrated by a significantly increased number of PI-positive nuclei 3h after the treatment (for ATG7: control vector: 2.6 ± 0.6%, ATG7-myc: 2.5 ± 1.1%, control vector KaHx: 43.3 ± 2.8%, ATG7-myc KaHx: 59.1 ± 3.3%, Steel-Dwass test; for BECN1: control vector: 2.6 ± 0.6%, BECN1-myc: 3.2 ± 1.2%, control vector KaHx: 43.3 ± 2.8%, BECN1-myc KaHx: 56.8 ± 5.4%, Tukey-Kramer test). Values are mean ± SEM expressed as a percentage of all nuclei (Hoechst-stained). n = 4 independent experiments. *p< 0.05, **p< 0.01, ***p< 0.001.

Figure 7. Neuronal autophagy is enhanced in the striatum after neonatal cerebral hypoxia-ischemia.

Cerebral hypoxia-ischemia (HI) increased the presence of neuronal autophagosomes in the striatum of 7-day old rats 24 h after HI as shown by **(A**) a higher level of LC3-II in immunoblots (sh: 100 ± 0%, 6 h: 121 ± 8%, n = 7 rats, 24 h: 166 ± 13%, n = 12 rats, Tukey-Kramer test) and **(B)** by strong punctate LC3-immunolabeling (arrows) in NeuN-positive neurons compared to sham-operated animals (sh). Bar = 20 µm. **(C)** Quantification of SQSTM1/P62 expression level by immunoblot shows that neonatal HI induces SQSTM1/P62 degradation (sh: 100 ± 4%, 24 h: 60 ± 7%, n = 8 rats, Welch ANOVA). Values are expressed as a percentage of sham-operated controls. **(D)** Neonatal cerebral HI increases β-hexosaminidase staining at 24 h compared to sham operated animals. Bar = 10 µm.

Figure 8. Inhibition of autophagy by lentiviral vectors expressing shRNA targeting BECLIN1 reduces brain damage following neonatal cerebral hypoxia-ischemia.

(A) Representative immunoblot and corresponding quantification showing that lentiviral injections mediating BECLIN1 (BECN1) downregulation decreased BECN1 expression levels by 30% compared to control lentiviral vector injections (control vector: 100 ± 7%, *Becn1* shRNA : 72 ± 10%), Welch ANOVA, n = 4 rats). When subjected to HI, animals injected with shRNA against *Becn1* present **(B)** a reduced induction of LC3-II expression 24 h after the insult (control vector: 100 ± 10, *Becn1* shRNA : 56 ± 12%, Welch ANOVA, n = 6 rats) and a decreased SQSTM1 degradation (control vector: 100 ± 4, *Becn1* shRNA : 112 ± 3%, Welch ANOVA, n = 8 rats). **(C)** Rat pups with striatal injection of *Becn1* shRNA show a higher percentage of "intact striatum", meaning surviving or non infarcted striatum, than do those with control vector-injection (control vector: 18 ± 2%, n=15; *Becn1* shRNA : 49 ± 7%, n = 12, Welch ANOVA). Values are mean ± SEM. *p< 0.05, **p< 0.01.

References

1. Klionsky DJ, Abdalla FC, Abeliovich H et al. Guidelines for the use and interpretation of assays for monitoring autophagy. Autophagy 2012; 8:445-544

2. Clarke PGH. Developmental cell death: morphological diversity and multiple mechanisms. Anat Embryol (Berl) 1990; 181:195-213

3. Puyal J., Ginet V., and Clarke P.G.H. Multiple interacting cell death mechanisms in the mediation of excitotoxicity and ischemic brain damage: A challenge for neuroprotection. Progress in Neurobiology 2013; 105:24-48

4. Clarke PGH, Puyal J. Autophagic cell death exists. Autophagy 2012; 8:867-869

5. Kroemer G, Levine B. Autophagic cell death: the story of a misnomer. Nat Rev Mol Cell Biol 2008; 9:1004-1010

6. Puyal J, Ginet V, Grishchuk Y et al. Neuronal Autophagy as a Mediator of Life and Death: Contrasting Roles in Chronic Neurodegenerative and Acute Neural Disorders. Neuroscientist 2012; 18:224-236

7. Wei K, Wang P, Miao CY. A Double-Edged Sword with Therapeutic Potential: An Updated Role of Autophagy in Ischemic Cerebral Injury. Cns Neuroscience & Therapeutics 2012; 18:879-886

8. Yuan JY, Kroemer G. Alternative cell death mechanisms in development and beyond. Genes Devel 2010; 24:2592-2602

9. Carloni S, Buonocore G, Balduini W. Protective role of autophagy in neonatal hypoxia-ischemia induced brain injury. Neurobiol Dis 2008; 32:329-339

10. Wang P, Guan YF, Du H et al. Induction of autophagy contributes to the neuroprotection of nicotinamide phosphoribosyltransferase in cerebral ischemic stroke. Autophagy 2012; 8:77-87

11. Koike M, Shibata M, Tadakoshi M et al. Inhibition of autophagy prevents hippocampal pyramidal neuron death after hypoxic-ischemic injury. Am J Pathol 2008; 172:454-469

12. Puyal J, Vaslin A, Mottier V et al. Postischemic treatment of neonatal cerebral ischemia should target autophagy. Ann Neurol 2009; 66:378-389

13. Wen YD, Sheng R, Zhang LS et al. Neuronal injury in rat model of permanent focal cerebral ischemia is associated with activation of autophagic and lysosomal pathways. Autophagy 2008; 4:762-769

14. Xing SH, Zhang YS, Li JJ et al. Beclin 1 knockdown inhibits autophagic activation and prevents secondary neurodegenerative damage in the ipsilateral thalamus following focal cerebral infarction. Autophagy 2012; 8:63-76

15. Rice JE, Vannucci RC, Brierley JB. The influence of immaturity on hypoxic-ischemic brain damage in the rat. Ann Neurol 1981; 9:131-141

16. Ginet V, Puyal J, Clarke PGH et al. Enhancement of autophagic flux after neonatal cerebral hypoxia-ischemia and its region-specific relationship to apoptotic mechanisms. Am J Pathol 2009; 175:1962-1974

17. Vincent P, Mulle C. Kainate Receptors in Epilepsy and Excitotoxicity. Neuroscience 2009; 158:309-323

18. Wang Q, Yu S, Simonyi A et al. Kainic acid-mediated excitotoxicity as a model for neurodegeneration. Molecular Neurobiology 2005; 31:3-16

19. Dong XX, Wang YR, Qin S et al. P53 Mediates Autophagy Activation and Mitochondria Dysfunction in Kainic Acid-Induced Excitotoxicity in Primary Striatal Neurons. Neuroscience 2012; 207:52-64

20. Shacka JJ, Lu J, Xie ZL et al. Kainic acid induces early and transient autophagic stress in mouse hippocampus. Neurosci Lett 2007; 414:57-60

21. Azad MB, Chen YQ, Gibson SB. Regulation of Autophagy by Reactive Oxygen Species (ROS): Implications for Cancer Progression and Treatment. Antioxidants & Redox Signaling 2009; 11:777-790

22. Chen Y, Azad MB, Gibson SB. Superoxide is the major reactive oxygen species regulating autophagy. Cell Death Differ 2009; 16:1040-1052

23. Szumiel I. Autophagy, reactive oxygen species and the fate of mammalian cells. Free Radical Research 2011; 45:253-265

24. Scherz-Shouval R, Weidberg H, Gonen C et al. p53-dependent regulation of autophagy protein LC3 supports cancer cell survival under prolonged starvation. Proceedings of the National Academy of Sciences of the United States of America 2010; 107:18511-18516

25. Wen YH, Zhai RG, Kim MD. The role of autophagy in Nmnat-mediated protection against hypoxia-induced dendrite degeneration. Mol Cell Neurosci 2013; 52:140-151

26. Yu L, Wan F, Dutta S et al. Autophagic programmed cell death by selective catalase degradation. Proc Natl Acad Sci U S A 2006; 103:4952-4957

27. Kubota C, Torii S, Hou N et al. Constitutive Reactive Oxygen Species Generation from Autophagosome/Lysosome in Neuronal Oxidative Toxicity. Journal of Biological Chemistry 2010; 285:667-674

28. Grishchuk Y, Ginet V, Truttmann AC et al. Beclin 1-independent autophagy contributes to apoptosis in cortical neurons. Autophagy 2011; 7:1115-1131

29. Kimura S, Noda T, Yoshimori T. Dissection of the autophagosome maturation process by a novel reporter protein, tandem fluorescent-tagged LC3. Autophagy 2007; 3:452-460

30. Borsello T, Croquelois K, Hornung JP et al. N-methyl-D-aspartate-triggered neuronal death in organotypic hippocampal cultures is endocytic, autophagic and mediated by the c-Jun N-terminal kinase pathway. Eur J Neurosci 2003; 18:473-485

31. Sadasivan S, Zhang ZQ, Larner SF et al. Acute NMDA toxicity in cultured rat cerebellar granule neurons is accompanied by autophagy induction and late onset autophagic cell death phenotype. Bmc Neuroscience 2010; 11

32. Matyja E, Taraszewska A, Naganska E et al. Autophagic degeneration of motor neurons in a model of slow glutamate excitotoxicity in vitro. Ultrastruct Pathol 2005; 29:331-339

33. Chang CF, Huang HJ, Lee HC et al. Melatonin attenuates kainic acid-induced neurotoxicity in mouse hippocampus via inhibition of autophagy and a-synuclein aggregation. Journal of Pineal Research 2012; 52:312-321

34. Wang Y, Han R, Liang ZQ et al. An autophagic mechanism is involved in apoptotic death of rat striatal neurons induced by the non-N-methyl-D-aspartate receptor agonist kainic acid. Autophagy 2008; 4:214-226

35. Wang Y, Gu ZL, Cao Y et al. Lysosomal enzyme cathepsin B is involved in kainic acid-induced excitotoxicity in rat striatum. Brain Res 2006; 1071:245-249

36. Adhami F, Liao GH, Morozov YM et al. Cerebral ischemia-hypoxia induces intravascular coagulation and autophagy. Amer J Pathol 2006; 169:566-583

37. Cui DR, Wang L, Qi AH et al. Propofol Prevents Autophagic Cell Death following Oxygen and Glucose Deprivation in PC12 Cells and Cerebral Ischemia-Reperfusion Injury in Rats. Plos One 2012; 7

38. Degterev A, Huang Z, Boyce M et al. Chemical inhibitor of nonapoptotic cell death with therapeutic potential for ischemic brain injury. Nature Chem Biol 2005; 1:112-119

39. Nitatori T, Sato N, Waguri S et al. Delayed neuronal death in the CA1 pyramidal cell layer of the gerbil hippocampus following transient ischemia is apoptosis. J Neurosci 1995; 15:1001-1011

40. Tian FF, Deguchi K, Yamashita T et al. In vivo imaging of autophagy in a mouse stroke model. Autophagy 2010; 6:1107-1114

41. Zhu C, Wang X, Xu F et al. The influence of age on apoptotic and other mechanisms of cell death after cerebral hypoxia-ischemia. Cell Death Differ 2005; 12:162-176

42. Xu F, Li J, Ni W et al. Peroxisome Proliferator-Activated Receptor-gamma Agonist 15d-Prostaglandin J(2) Mediates Neuronal Autophagy after Cerebral Ischemia-Reperfusion Injury. Plos One 2013; 8

43. Puyal J, Clarke PGH. Targeting autophagy to prevent neonatal stroke damage. Autophagy 2009; 5:1060-1061

44. Liu Y, Shoji-Kawata S, Sumpter RM Jr et al. Autosis is a Na+,K+-ATPase-regulated form of cell death triggered by autophagy-inducing peptides, starvation, and hypoxia-ischemia. Proc Natl Acad Sci U S A. 2013 (in press) doi/10.1073/pnas.1319661110

45. Perez-Carrion MD, Perez-Martinez FC, Merino S et al. Dendrimer-mediated siRNA delivery knocks down Beclin 1 and potentiates NMDA-mediated toxicity in rat cortical neurons. Journal of Neurochemistry 2012; 120:259-268

46. Carloni S, Buonocore G, Longini M et al. Inhibition of rapamycin-induced autophagy causes necrotic cell death associated with Bax/Bad mitochondrial translocation. Neuroscience 2012; 203:160-9.

47. Carloni S, Girelli S, Scopa C et al. Activation of autophagy and Akt/CREB signaling play an equivalent role in the neuroprotective effect of rapamycin in neonatal hypoxia-ischemia. Autophagy 2010; 6:366-77.

48. Papadakis M, Hadley G, Xilouri M et al. Tsc1 (hamartin) confers neuroprotection against ischemia by inducing autophagy. Nature Medicine 2013; 19:351-7.

49. Sheng R, Zhang LS, Han R et al. Autophagy activation is associated with neuroprotection in a rat model of focal cerebral ischemic preconditioning. Autophagy 2010; 6:482-94.

50. Hughes KJ, Kennedy BK. Rapamycin Paradox Resolved. Science 2012; 335:1578-1579

51. Wu YT, Tan HL, Shui G et al. Dual role of 3-methyladenine in modulation of autophagy via different temporal patterns of inhibition on class I and III phosphoinositide 3-kinase. J Biol Chem 2010; 285:10850-10861

52. Tiede LM, Cook EA, Morsey B et al. Oxygen matters: tissue culture oxygen levels affect mitochondrial function and structure as well as responses to HIV viroproteins. Cell Death Dis. 2011; 22;2:e246.

53. Oh S, Shin CS, Kim HS. The time course of NMDA- and Kainate-induced cGMP elevation and glutamate release in cultured neuron. Arch Pharm Res 1995; 18:153-158.

54. Chen J, Li C, Pei DS et al. GluR6-containing KA receptor mediates the activation of p38 MAP kinase in rat hippocampal CA1 region during brain ischemia injury. Hippocampus 2009; 19:79-89.

55. Lowry ER, Kruyer A, Norris EH et al. The GluK4 kainate receptor subunit regulates memory, mood, and excitotoxic neurodegeneration. Neuroscience 2013; 235:215-25.

56. Schurr A, Rigor BM. Quinolinate Potentiates the Neurotoxicity of Excitatory Amino-Acids in Hypoxic Neuronal Tissue In-Vitro. Brain Research 1993; 617:76-80

57. Schurr A, Payne RS, Rigor BM. Protection by Mk-801 Against Hypoxia-Induced, Excitotoxin-Induced, and Depolarization-Induced Neuronal Damage In-Vitro. Neurochemistry International 1995; 26:519-525

58. Mishra OP, Kubin JA, McGowan JE et al. Kainate receptor modification in the fetal guinea pig brain during hypoxia. Neurochemical Research 1995; 20:1171-1177

59. Panigrahy A, White WF, Rava LA et al. Developmental changes in [3H]kainate binding in human brainstem sites vulnerable to perinatal hypoxia-ischemia. Neuroscience 1995; 67:441-54.

60. Lau A, Tymianski M. Glutamate receptors, neurotoxicity and neurodegeneration. Pflugers Arch 2010; 460:525-42.

61. Wang Y, Qin ZH. Molecular and cellular mechanisms of excitotoxic neuronal death. Apoptosis 2010; 15:1382-402.

62. Sakaida I, Kyle ME, Farber JL. Autophagic Degradation of Protein Generates A Pool of Ferric Iron Required for the Killing of Cultured-Hepatocytes by An Oxidative Stress. Molecular Pharmacology 1990; 37:435-442

63. Seyfried D, Han YX, Zheng Z et al. Cathepsin B and middle cerebral artery occlusion in the rat. J Neurosurg 1997; 87:716-723

64. Hara T, Nakamura K, Matsui M et al. Suppression of basal autophagy in neural cells causes neurodegenerative disease in mice. Nature 2006; 441:885–9.

65. Komatsu M, Waguri S, Chiba T et al. Loss of autophagy in the central nervous system causes neurodegeneration in mice. Nature 2006; 441:880–4.

66. Vaslin A, Puyal J, Borsello T et al. Excitotoxicity-related endocytosis in cortical neurons. J Neurochem 2007; 102:789-800

67. Levine S. Anoxic-Ischemic Encephalopathy in Rats. Journal of Neuropathology and Experimental Neurology 1960; 19:165-166

68. Ginet V, Puyal J, Magnin G et al. Limited role of the c-Jun N-terminal kinase pathway in a neonatal rat model of cerebral hypoxia-ischemia. J Neurochem 2009; 108:552-562

69. Vaslin A, Puyal J, Clarke PGH. Excitotoxicity-induced endocytosis confers drug targeting in cerebral ischemia. Ann Neurol 2009; 65:337-347

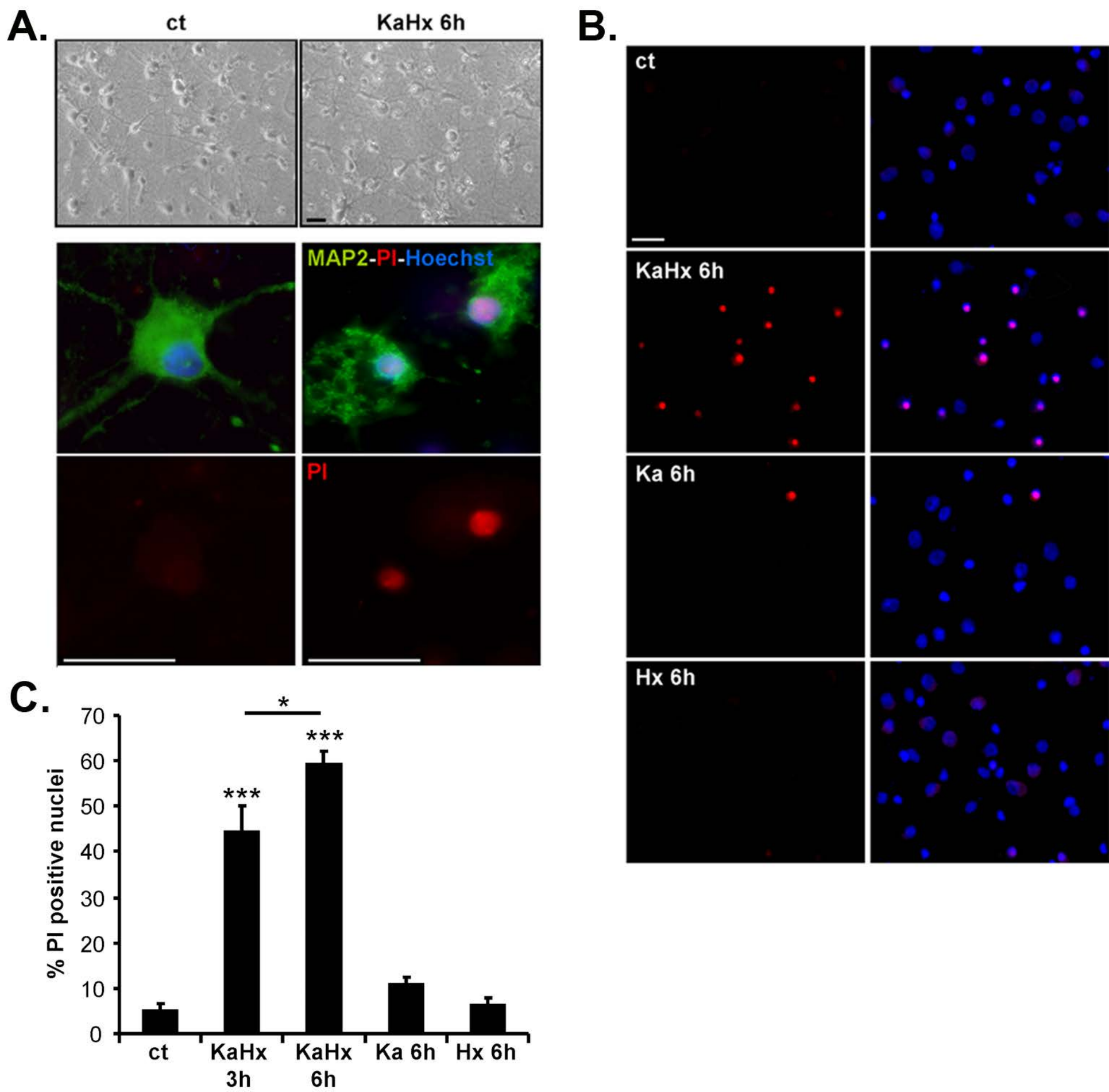
A.
ct
KaHx 6h
MAP2-PI-Hoechst
PI
B.
ct
KaHx 6h
Ka 6h
Hx 6h
C.
% PI positive nuclei
70
60
50
40
30
20
10
0
*
***
***
ct
KaHx 3h
KaHx 6h
Ka 6h
Hx 6h

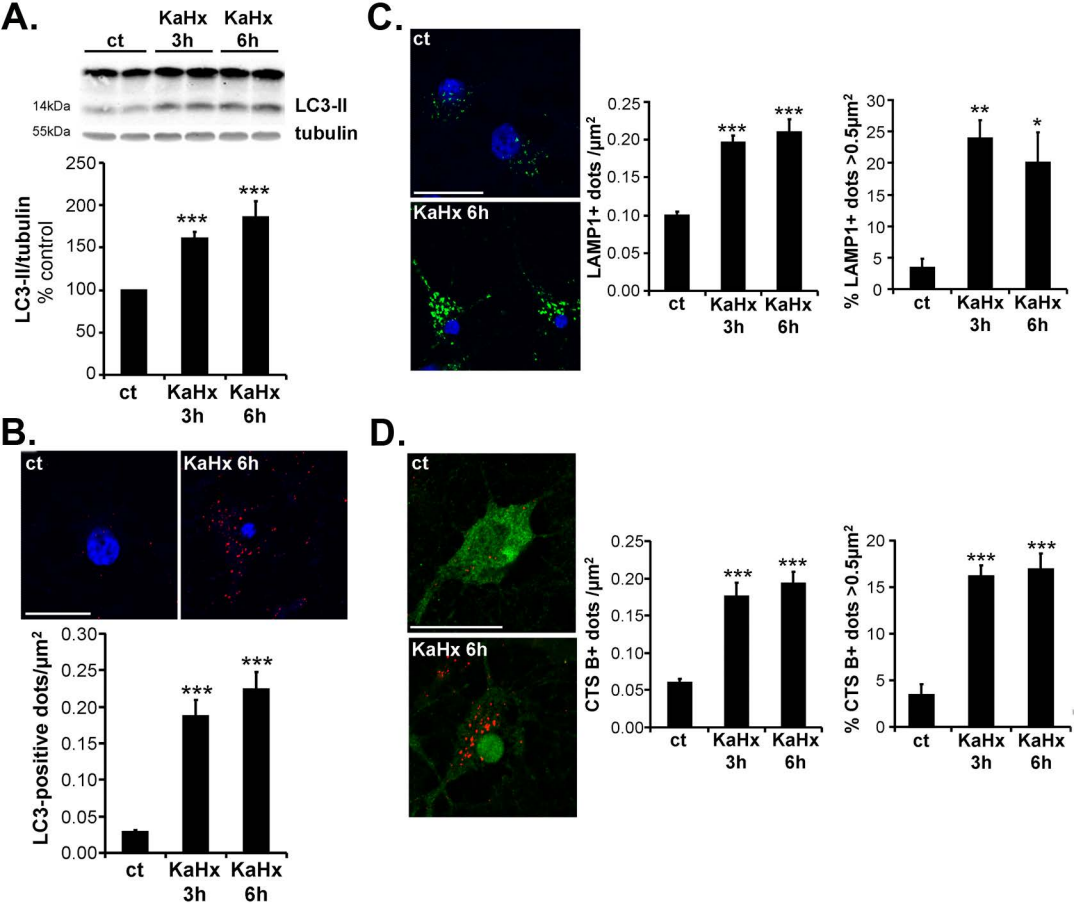
A.
ct
KaHx 3h
KaHx 6h
14kDa
55kDa
LC3-II
tubulin
LC3-II/tubulin % control
250
200
150
100
50
0
***
***
ct
KaHx 3h
KaHx 6h
B.
ct
KaHx 6h
LC3-positive dots/µm²
0.30
0.25
0.20
0.15
0.10
0.05
0.00
***
***
ct
KaHx 3h
KaHx 6h
C.
ct
KaHx 6h
LAMP1+ dots /µm²
0.25
0.20
0.15
0.10
0.05
0.00
***
***
ct
KaHx 3h
KaHx 6h
% LAMP1+ dots >0.5µm²
30
25
20
15
10
5
0
**
*
ct
KaHx 3h
KaHx 6h
D.
ct
KaHx 6h
CTS B+ dots /µm²
0.25
0.20
0.15
0.10
0.05
0.00
***
***
ct
KaHx 3h
KaHx 6h
% CTS B+ dots >0.5µm²
20
15
10
5
0
***
***
ct
KaHx 3h
KaHx 6h

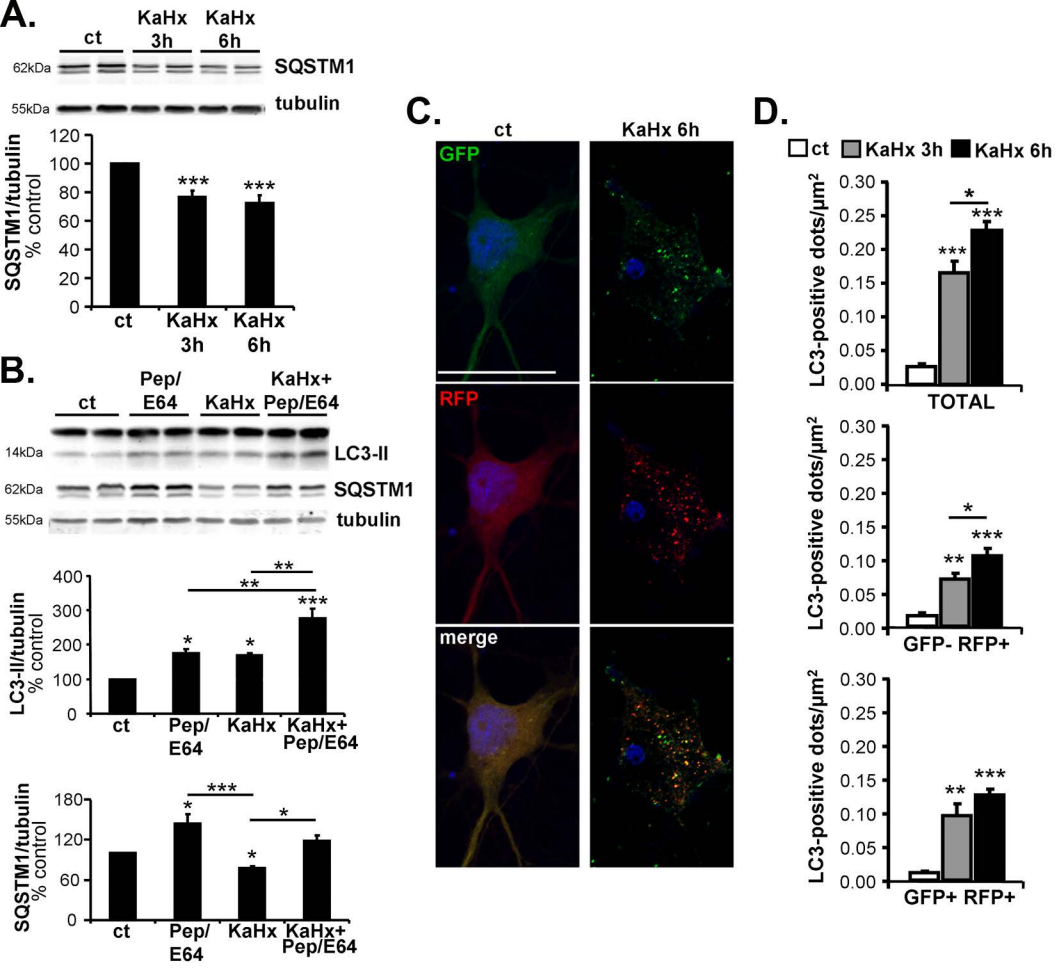
A.
ct
KaHx 3h
KaHx 6h
62kDa
SQSTM1
55kDa
tubulin
SQSTM1/tubulin % control
120
100
80
60
40
20
0
***
***
ct
KaHx 3h
KaHx 6h
B.
ct
Pep/ E64
KaHx
KaHx+ Pep/E64
14kDa
LC3-II
62kDa
SQSTM1
55kDa
tubulin
LC3-II/tubulin % control
400
300
200
100
0
*
*
**
**
***
ct
Pep/ E64
KaHx
KaHx+ Pep/E64
SQSTM1/tubulin % control
180
120
60
0
*
*
*
***
*
ct
Pep/ E64
KaHx
KaHx+ Pep/E64
C.
ct
KaHx 6h
GFP
RFP
merge
D.
ct
KaHx 3h
KaHx 6h
LC3-positive dots/µm²
0.30
0.25
0.20
0.15
0.10
0.05
0.00
*
***
***
TOTAL
LC3-positive dots/µm²
0.30
0.25
0.20
0.15
0.10
0.05
0.00
*
**
***
GFP- RFP+
LC3-positive dots/µm²
0.30
0.25
0.20
0.15
0.10
0.05
0.00
**
***
GFP+ RFP+

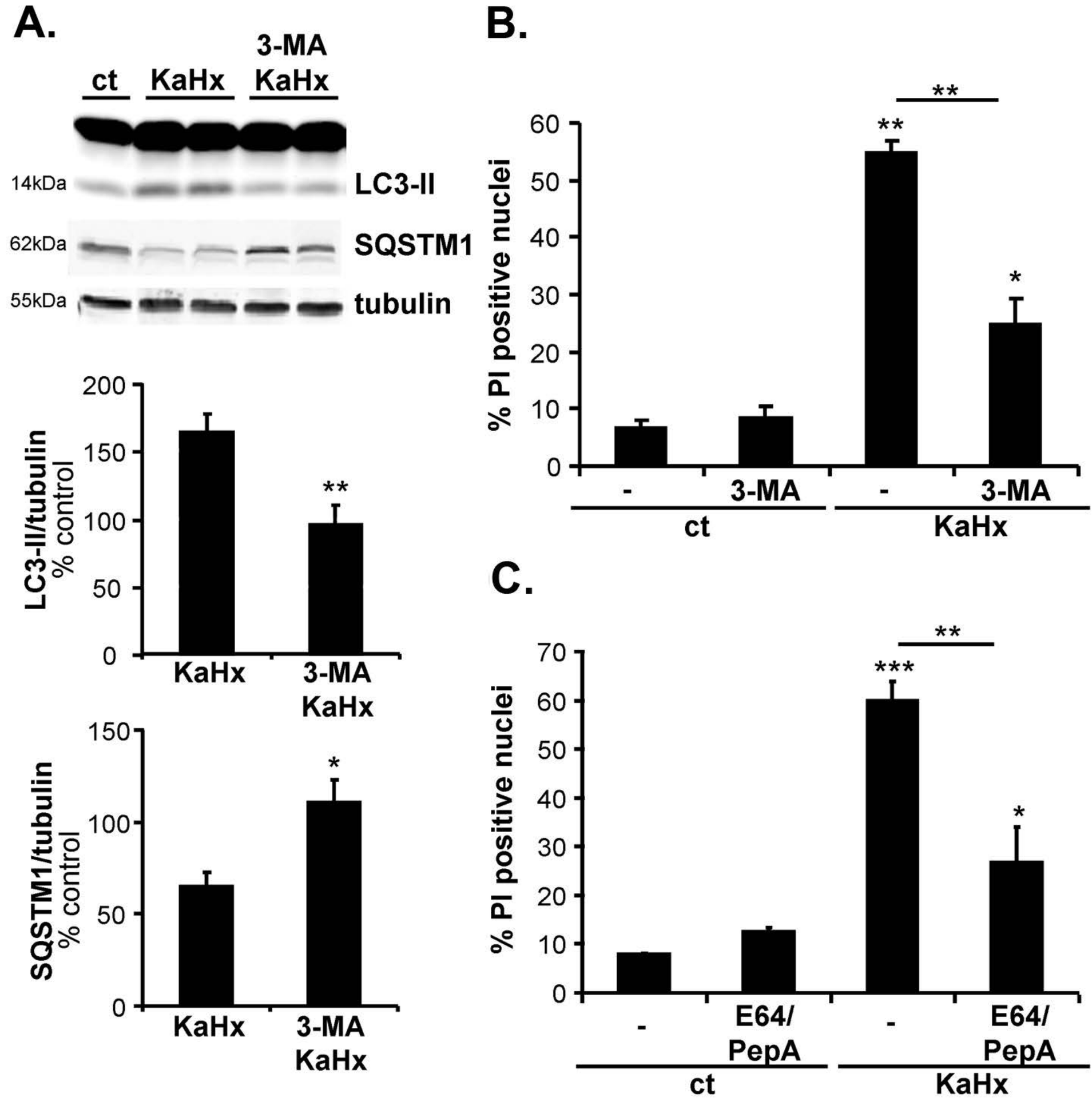
A.
ct
KaHx
3-MA KaHx
14kDa
LC3-II
62kDa
SQSTM1
55kDa
tubulin
LC3-II/tubulin % control
200
150
100
50
0
**
KaHx
3-MA KaHx
SQSTM1/tubulin % control
150
100
50
0
*
KaHx
3-MA KaHx
B.
% PI positive nuclei
60
50
40
30
20
10
0
**
**
*
-
3-MA
-
3-MA
ct
KaHx
C.
% PI positive nuclei
70
60
50
40
30
20
10
0
**
***
*
-
E64/ PepA
-
E64/ PepA
ct
KaHx

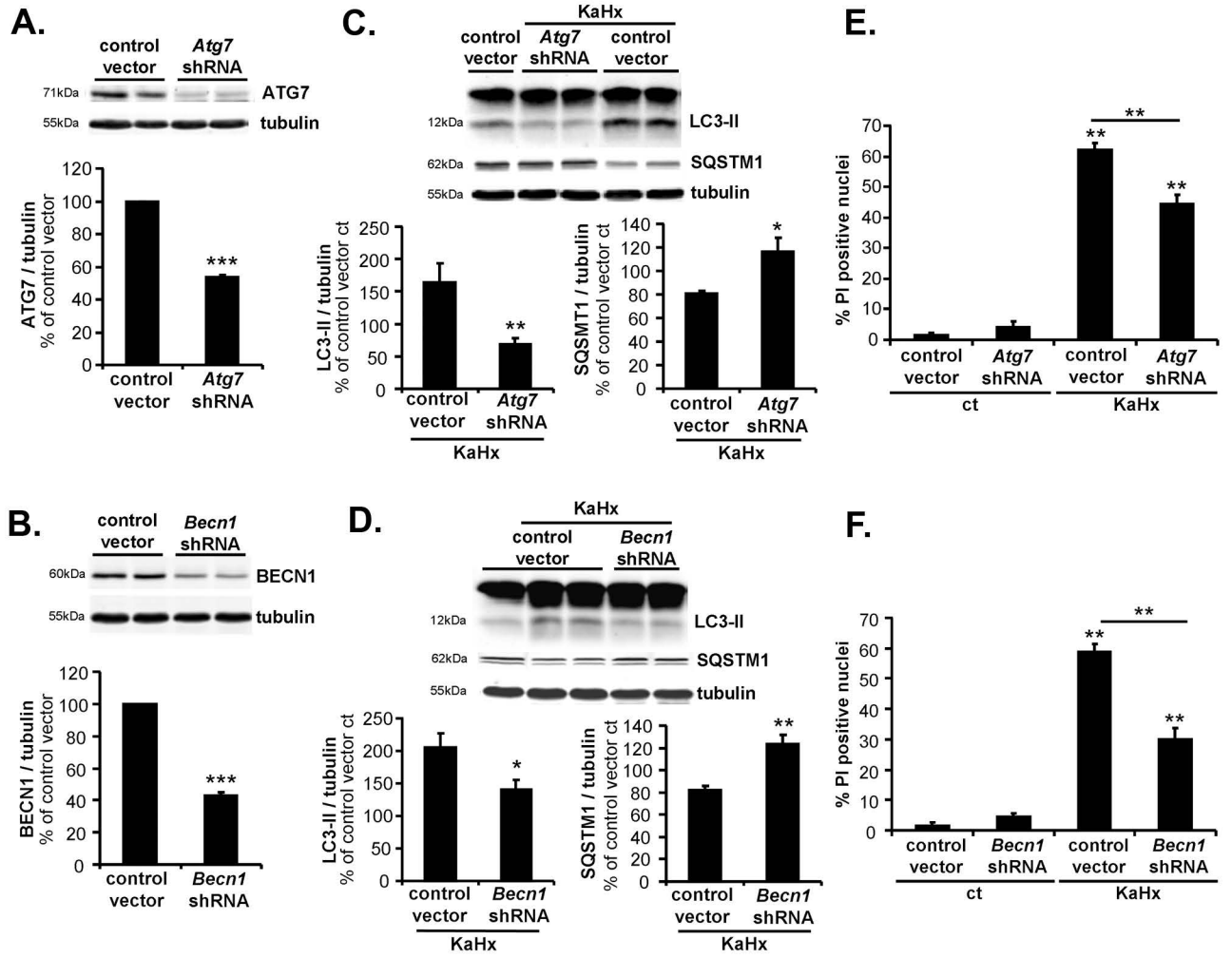
A.
control vector
Atg7 shRNA
71kDa
ATG7
55kDa
tubulin
ATG7 / tubulin % of control vector
***
control vector
Atg7 shRNA
B.
control vector
Becn1 shRNA
60kDa
BECN1
55kDa
tubulin
BECN1 / tubulin % of control vector
***
control vector
Becn1 shRNA
C.
KaHx
control vector
Atg7 shRNA
control vector
12kDa
LC3-II
62kDa
SQSTM1
55kDa
tubulin
LC3-II / tubulin % of control vector ct
**
SQSTM1 / tubulin % of control vector ct
*
control vector
Atg7 shRNA
KaHx
D.
KaHx
control vector
Becn1 shRNA
12kDa
LC3-II
62kDa
SQSTM1
55kDa
tubulin
LC3-II / tubulin % of control vector ct
*
SQSTM1 / tubulin % of control vector ct
**
control vector
Becn1 shRNA
KaHx
E.
% PI positive nuclei
**
**
**
control vector
Atg7 shRNA
control vector
Atg7 shRNA
ct
KaHx
F.
% PI positive nuclei
**
**
**
control vector
Becn1 shRNA
control vector
Becn1 shRNA
ct
KaHx

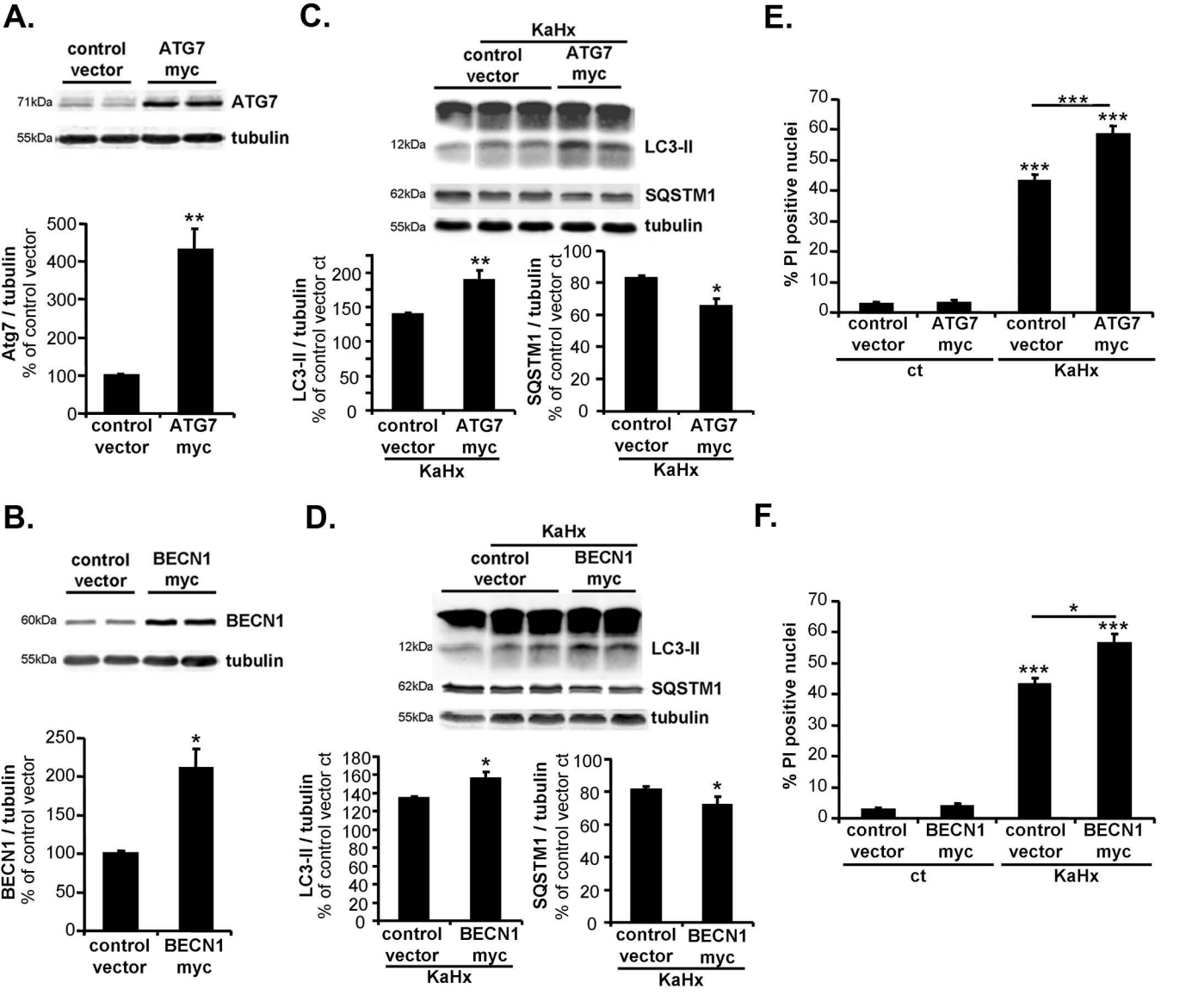
A.
control vector
ATG7 myc
71kDa
ATG7
55kDa
tubulin
Atg7 / tubulin % of control vector
control vector
ATG7 myc
B.
control vector
BECN1 myc
60kDa
BECN1
55kDa
tubulin
BECN1 / tubulin % of control vector
control vector
BECN1 myc
C.
KaHx
control vector
ATG7 myc
12kDa
LC3-II
62kDa
SQSTM1
55kDa
tubulin
LC3-II / tubulin % of control vector ct
SQSTM1 / tubulin % of control vector ct
control vector
ATG7 myc
KaHx
D.
KaHx
control vector
BECN1 myc
12kDa
LC3-II
62kDa
SQSTM1
55kDa
tubulin
LC3-II / tubulin % of control vector ct
SQSTM1 / tubulin % of control vector ct
control vector
BECN1 myc
KaHx
E.
% PI positive nuclei
control vector
ATG7 myc
control vector
ATG7 myc
ct
KaHx
F.
% PI positive nuclei
control vector
BECN1 myc
control vector
BECN1 myc
ct
KaHx

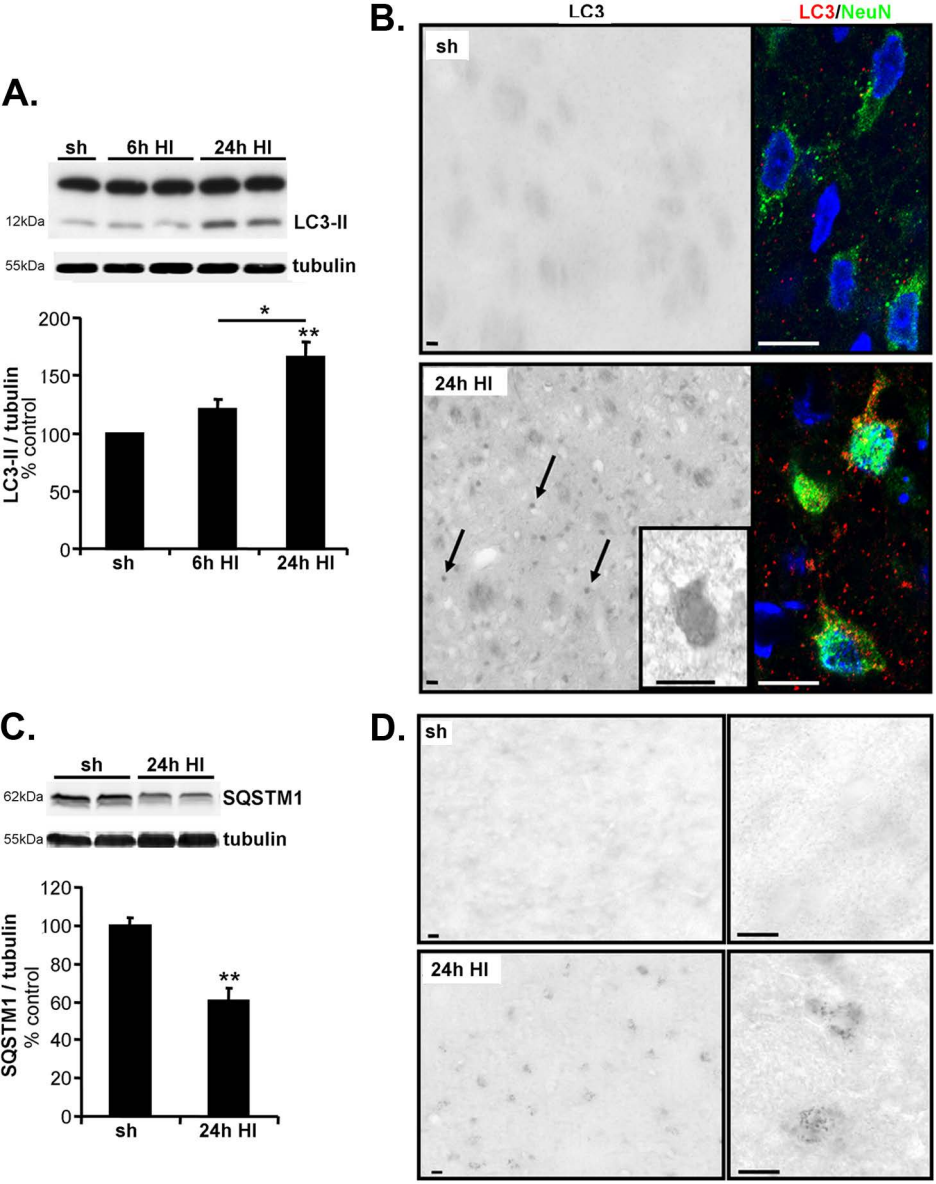
A.
sh
6h HI
24h HI
12kDa
LC3-II
55kDa
tubulin
LC3-II / tubulin
% control
200
150
100
50
0
*
**
sh
6h HI
24h HI
B.
LC3
LC3/NeuN
sh
24h HI
C.
sh
24h HI
62kDa
SQSTM1
55kDa
tubulin
SQSTM1 / tubulin
% control
120
100
80
60
40
20
0
**
sh
24h HI
D.
sh
24h HI

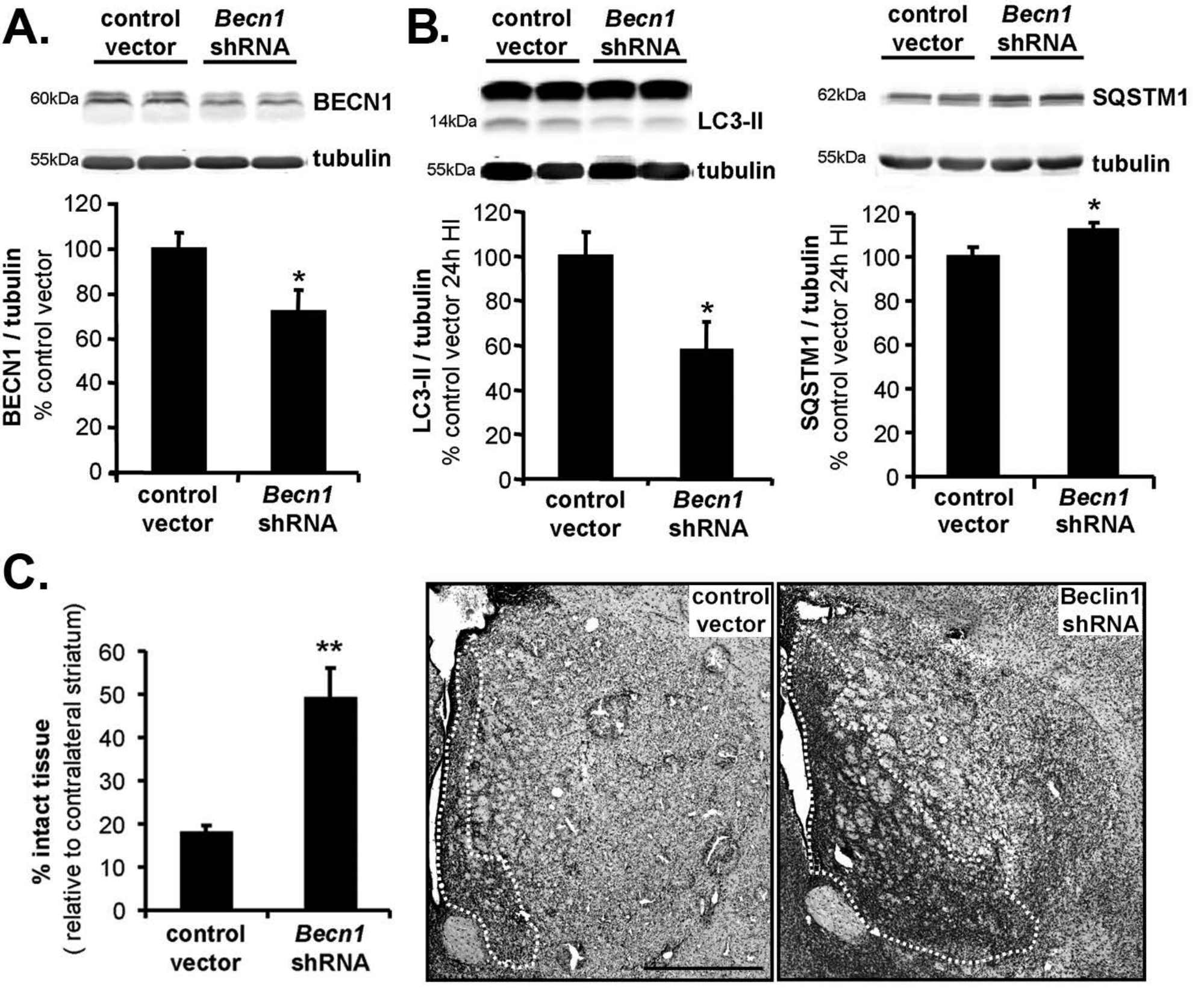
A.
control vector
Becn1 shRNA
60kDa
BECN1
55kDa
tubulin
BECN1 / tubulin
% control vector
120
100
80
60
40
20
0
*
control vector
Becn1 shRNA
B.
control vector
Becn1 shRNA
14kDa
LC3-II
55kDa
tubulin
LC3-II / tubulin
% control vector 24h HI
120
100
80
60
40
20
0
*
control vector
Becn1 shRNA
control vector
Becn1 shRNA
62kDa
SQSTM1
55kDa
tubulin
SQSTM1 / tubulin
% control vector 24h HI
120
100
80
60
40
20
0
*
control vector
Becn1 shRNA
C.
% intact tissue
(relative to contralateral striatum)
60
50
40
30
20
10
0
**
control vector
Becn1 shRNA
control vector
Beclin1 shRNA

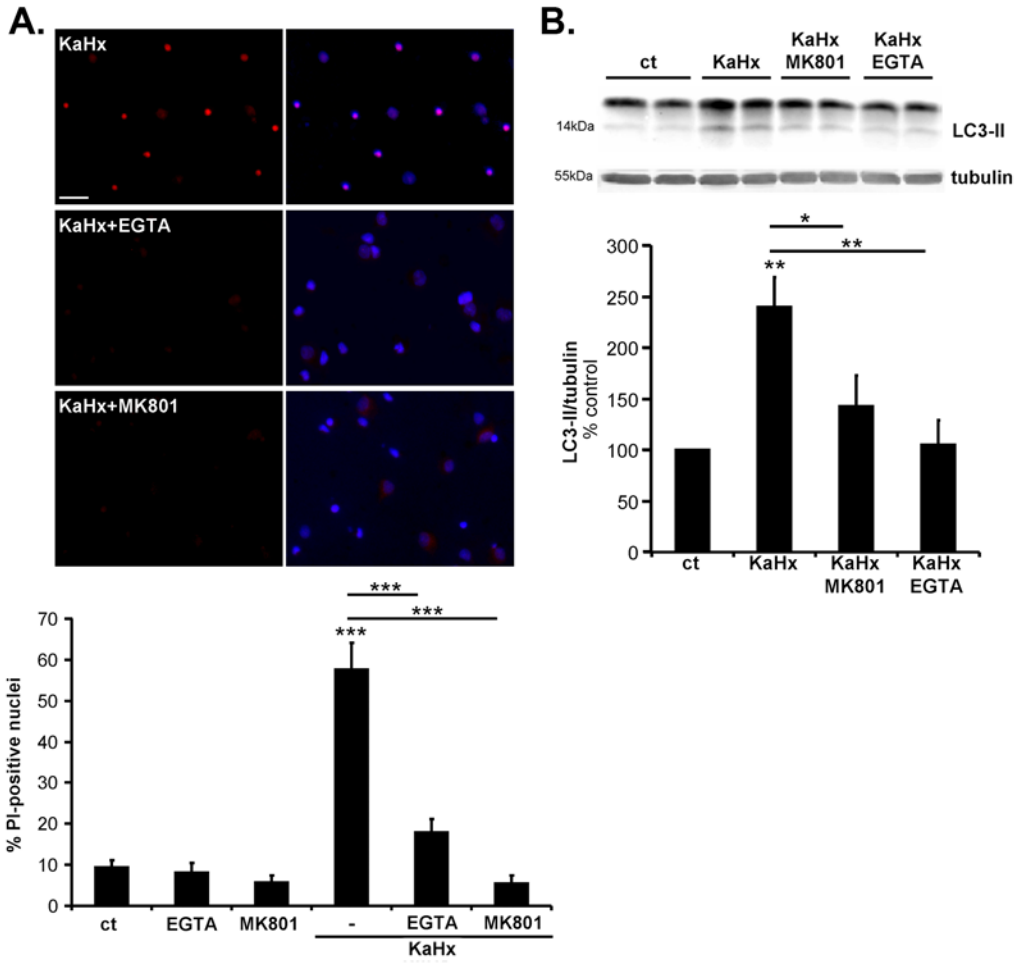

Figure S1. Kainate/hypoxia-induced neuronal death is calcium dependent and mediated by NMDA receptors.

(A) Quantification of PI-positive nuclei as a percentage of all nuclei showing that kainate/hypoxia (KaHx)-induced cell death is prevented when neurons are treated with either EGTA (chelator of extracellular calcium) or the NMDA receptor antagonist MK801. (ct: 9 ± 2%; EGTA: 8 ± 2.%; MK801: 6 ± 2%, KaHx: 58 ± 7%; KaHx+EGTA:

18 ± 3%; KaHx+MK801: 6 ± 2%). Steel-Dwass test. n = 6 independent experiments. **(B)** Representative immunoblot of LC3 (upper part) and the corresponding quantification (lower part) showing that the increase of LC3-II induced by KaHx does not occur in presence of EGTA and MK801. (KaHx: 240 ± 29%, KaHx+MK801: 143 ± 30%, KaHx+EGTA: 105 ± 24%). Steel-Dwass test. n = 5 independent experiments. Values are mean ± SEM, *p < 0.05, **p< 0.01, ***p< 0.001.

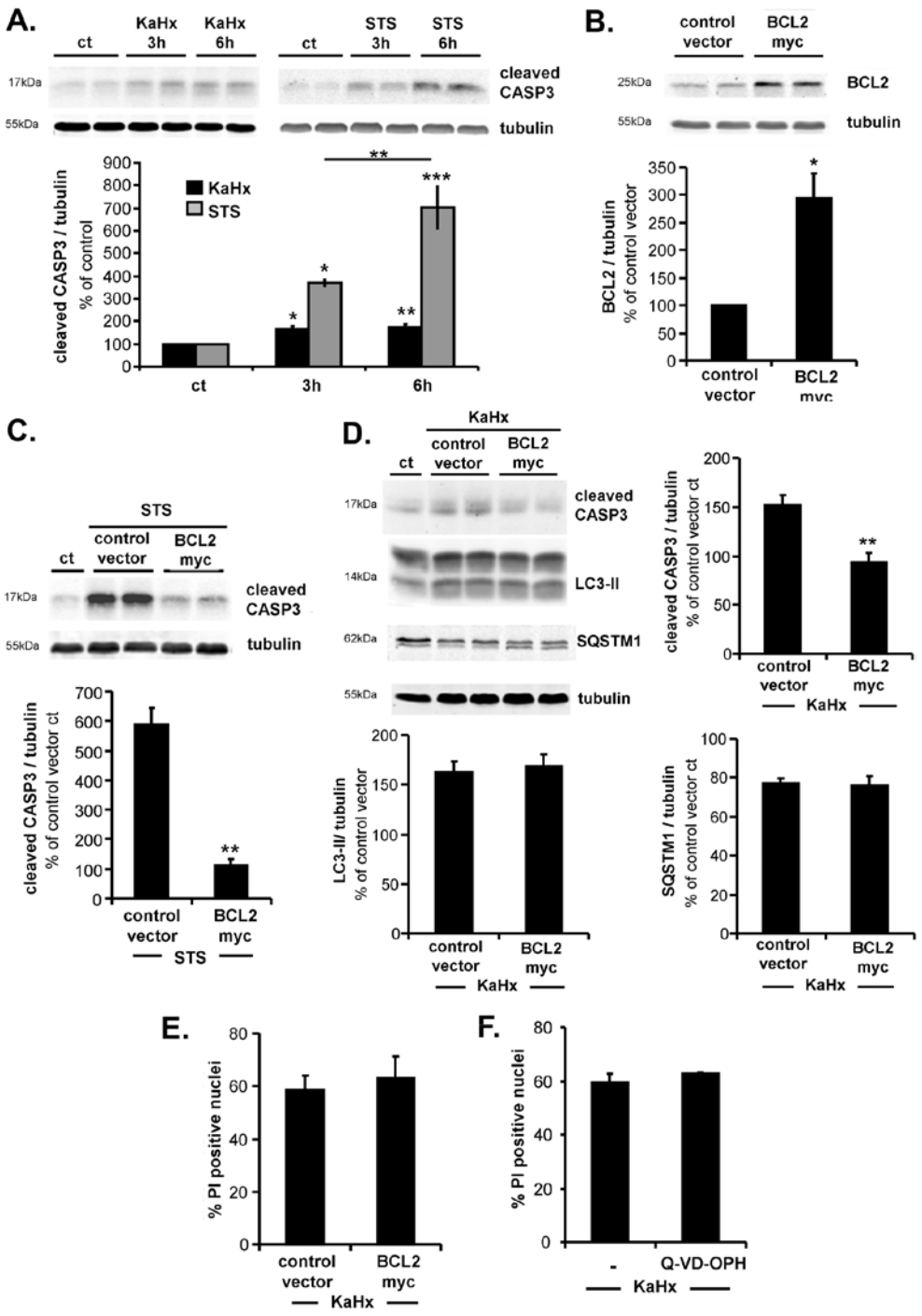

Figure S2. Kainate/hypoxia-induced neuronal death is caspase-independent.

(A) Comparison between the activation of CASPASE (CASP)-3 at 3 h and 6 h after kainate/hypoxia (KaHx) stimulation and after staurosporine (STS) exposure (1 μM) indicates that the KaHx model involves much less activation of CASP-3 than does the

STS model, as shown by representative immunoblots and corresponding quantifications. (for KaHx: 3 h: 163 ± 14%, 6 h: 172 ± 14%; for STS: 3 h: 369 ± 19%, 6 h: 703 ± 100%). Values are mean ± SEM expressed as a percentage of control treatment (30 min in BBS medium for KaHx and 0.1% DMSO for STS). *p < 0.05, **p<0.01, ***p< 0.001, Steel-Dwaas test. n = 4 independent experiments. **(B)** Lentiviral transduction of cultured cortical neurons with BCL2-myc induces a strong overexpression of BCL2 (BCL2-myc: 295 ± 43%). Values are mean ± SEM expressed as a percentage of neurons transduced with control vector. *p<0.05, Wilcoxon test. n = 4 independent experiments. **(C)** Overexpression of BCL2 completely prevents CASP-3 activation induced by 6 h of STS (control vector: 589 ± 58%, BCL2-myc: 111 ± 22%). Values are mean ± SEM expressed as a percentage of neurons transduced with control vector and treated with DMSO. ***p<0.001, Welch ANOVA. n = 4 independent experiments. **(D)** Overexpression of BCL2 blocks KaHx-induced CASP-3 activation (control vector KaHx: 152 ± 10%, BCL2-myc KaHx: 93 ± 10%) but does not affect LC3-II (control vector KaHx: 162 ± 17%, BCL2-myc KaHx: 168 ± 12%) or SQSTM1/P62 (control vector KaHx: 77 ± 3%, BCL2-myc KaHx: 76 ± 5%) expression. Values are mean ± SEM expressed as a percentage of neurons transduced with control vector after control stimulation. **p<0.01, Welch ANOVA. n = 4 independent experiments. (**E-F**) Caspase-inhibtion by **(E)** BCL2-myc lentiviral transduction (control vector KaHx: 59 ± 5%, BCL2-myc KaHx: 63 ± 8%) or **(F)** by Q-VD-OPH pre-treatment (control KaHx: 59 ± 4%, Q-VD-OPH KaHx: 63 ± 1%) is not neuroprotective, as is demonstrated by quantification of PI-positive nuclei. Values are mean ± SEM expressed as a percentage of all nuclei (Hoechst-stained). n = 4 independent experiments.

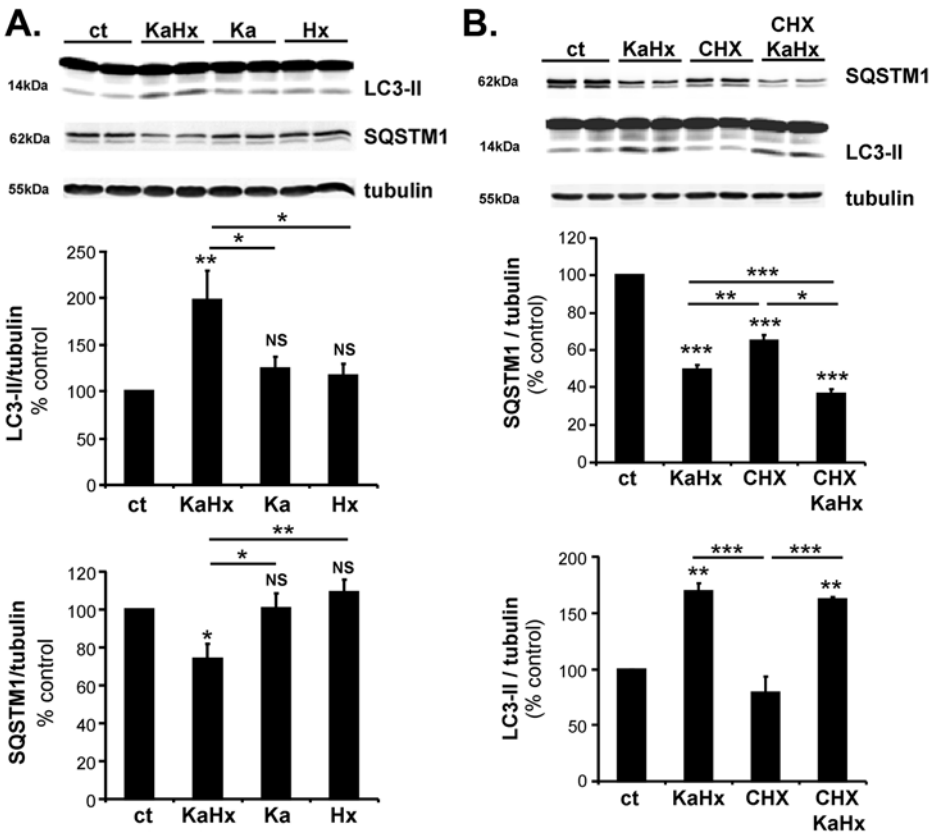

Figure S3. Kainate and hypoxia alone does not enhance autophagy.

(A) LC3 and SQSTM1 representative immunoblots and the corresponding quantifications showing that LC3-II expression level is upregulated (KaHx: 198 ± 32%) and SQSTM1 is decreased (KaHx: 74 ± 8%) at 6 h after kainate/hypoxia (KaHx) stimulation whereas both treatments have no significant (NS) effect separately (for LC3-II: Ka: 125 ± 12%, Hx: 116 ± 13%, Steel-Dwaas test; for SQSTM1: Ka: 101 ± 8%, Hx: 109 ± 7%, Tukey-Kramer test). Values are mean ± SEM. ***p< 0.001. n = 7 independent experiments. **(B)** Representative immunoblots for SQSTM1 and LC3, and the corresponding quantifications, demonstrating that kainate/hypoxia (KaHx)-induced SQSTM1 decrease persists even in the presence of a protein synthesis inhibitor (1µg/µl cycloheximide, CHX, 1h of pre-treatment) (KaHx 6 h: 50 ± 2%, CHX: 65 ± 3%, CHX+KaHx 6 h: 36 ± 3%). Increase in LC3-II expression is not affected by CHX during the first 6 h (KaHx 6

h: 169 ± 8%, CHX: 79 ± 14%, CHX+KaHx 6 h: 162 ± 2%). Values are mean ± SEM. ***p< 0.001, Tukey-Kramer test. n = 3 independent experiments.

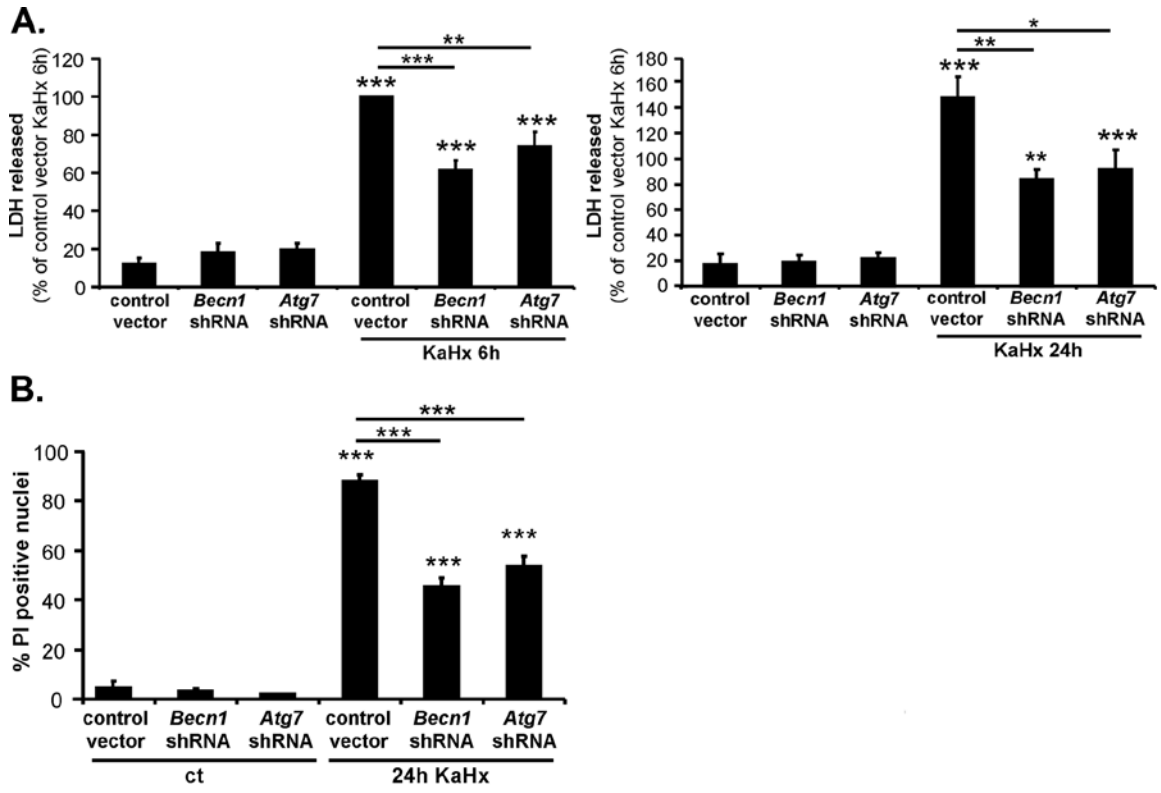

Figure S4. Inhibition of autophagy by downregulation of ATG7 or BECLIN1 protects cultured cortical neurons 24 h after kainate/hypoxia treatment.

(A) Neuroprotective effect of downregulation of ATG7 and BECN1 as shown by the quantification of the lactate deshydrogenase (LDH) release in the medium at both 6 h (6 h: control vector: 12 ± 3%, *Becn1* shRNA: 17 ± 6%, *Atg7* shRNA: 19 ± 3%, control vector KaHx: 100 ± 0%, *Becn1* shRNA KaHx: 61 ± 5%, *Atg7* shRNA KaHx: 74 ± 8%) and 24 h (control vector: 17 ± 8%, *Becn1* shRNA: 19 ± 5%, *Atg7* shRNA: 21 ± 5%, control vector KaHx: 146 ± 17%, *Becn1* shRNA KaHx: 85 ± 8%, *Atg7* shRNA KaHx: 93 ± 15%). Values are mean ± SEM expressed as a percentage of the value reached by control vector infected neurons 6h after KaHx. *p<0.05, **p<0.01, ***p< 0.001, Steel-Dwass test, n = 5 independent experiments. **(B)** Transduced neurons with *Atg7* and

Beclin) (*Becn1)* shRNAs are less sensitive to kainate/hypoxia (KaHx) than control vector transduced neurons as demonstrated by a significant decreased number of propidium iodide (PI)-positive nuclei 24 h after the stimulation (control vector: 5 ± 3%, *Becn1* shRNA: 3 ± 1%, *Atg7* shRNA: 2 ± 0.1%, control vector KaHx: 88 ± 2%, *Becn1* shRNA KaHx: 45 ± 4%, *Atg7* shRNA KaHx: 53 ± 4%). Values are mean ± SEM expressed as a percentage of all nuclei (Hoechst-stained). ***p< 0.001, Steel-Dwass test, n = 6 independent experiments.

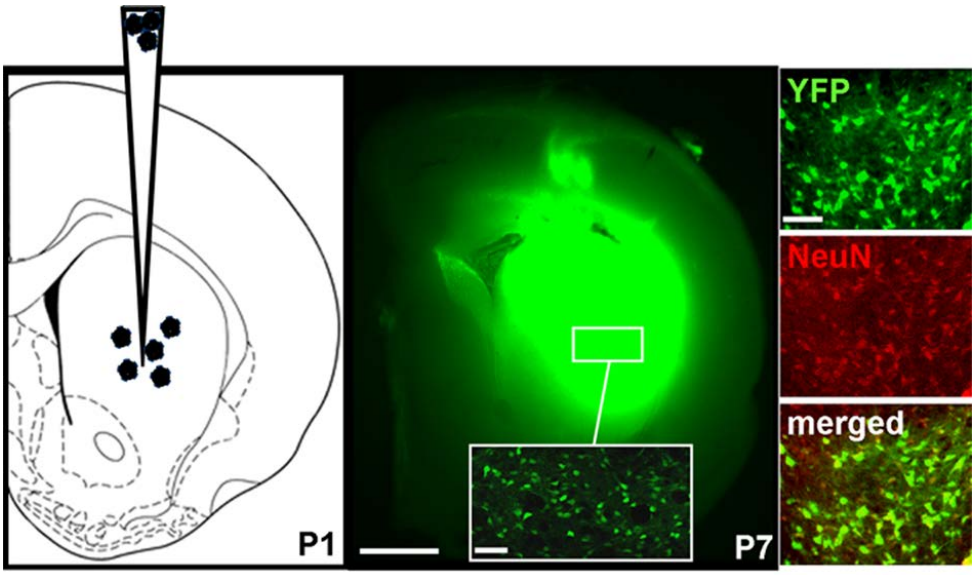

Figure S5. Intrastriatal lentiviral vector injection.

Lentiviral vectors stereotaxically injected in the right striatum of 1 or 2-day old rat pups infected most of the striatal neurons as demonstrated with a vector transducing a yellow fluorescent protein (YFP) (green) 5 days after injection and immunolabelling with the neuronal marker NeuN (red). Low magnification of the entire hemisphere was done with a stereomicroscope with fluorescence and high magnifications are confocal images.

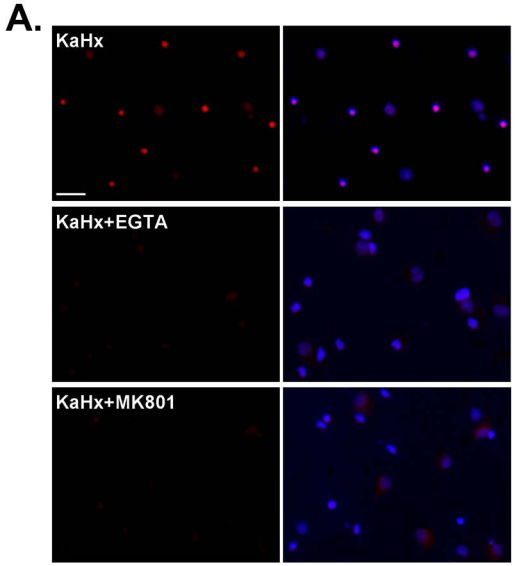
A.
KaHx
KaHx+EGTA
KaHx+MK801

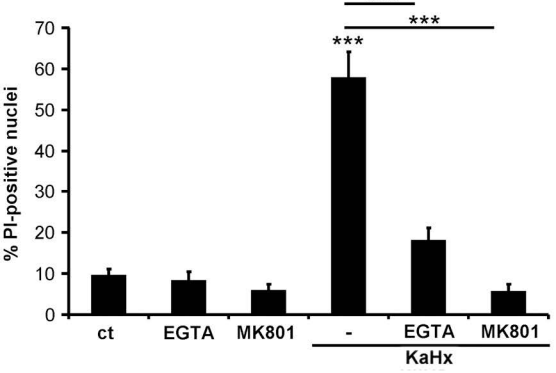
***
***
***
70
60
50
40
30
20
10
0
% PI-positive nuclei
ct
EGTA
MK801
-
EGTA
MK801
KaHx

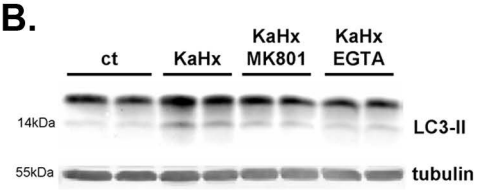
B.
ct
KaHx
KaHx MK801
KaHx EGTA
14kDa
LC3-II
55kDa
tubulin

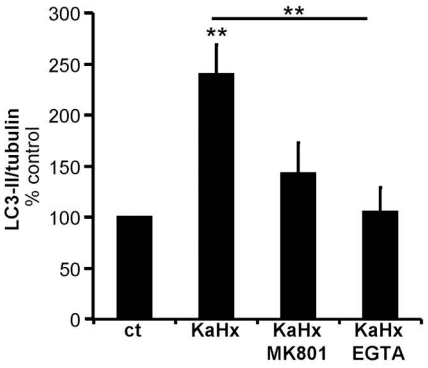
*
**
**
300
250
200
150
100
50
0
LC3-II/tubulin % control
ct
KaHx
KaHx MK801
KaHx EGTA

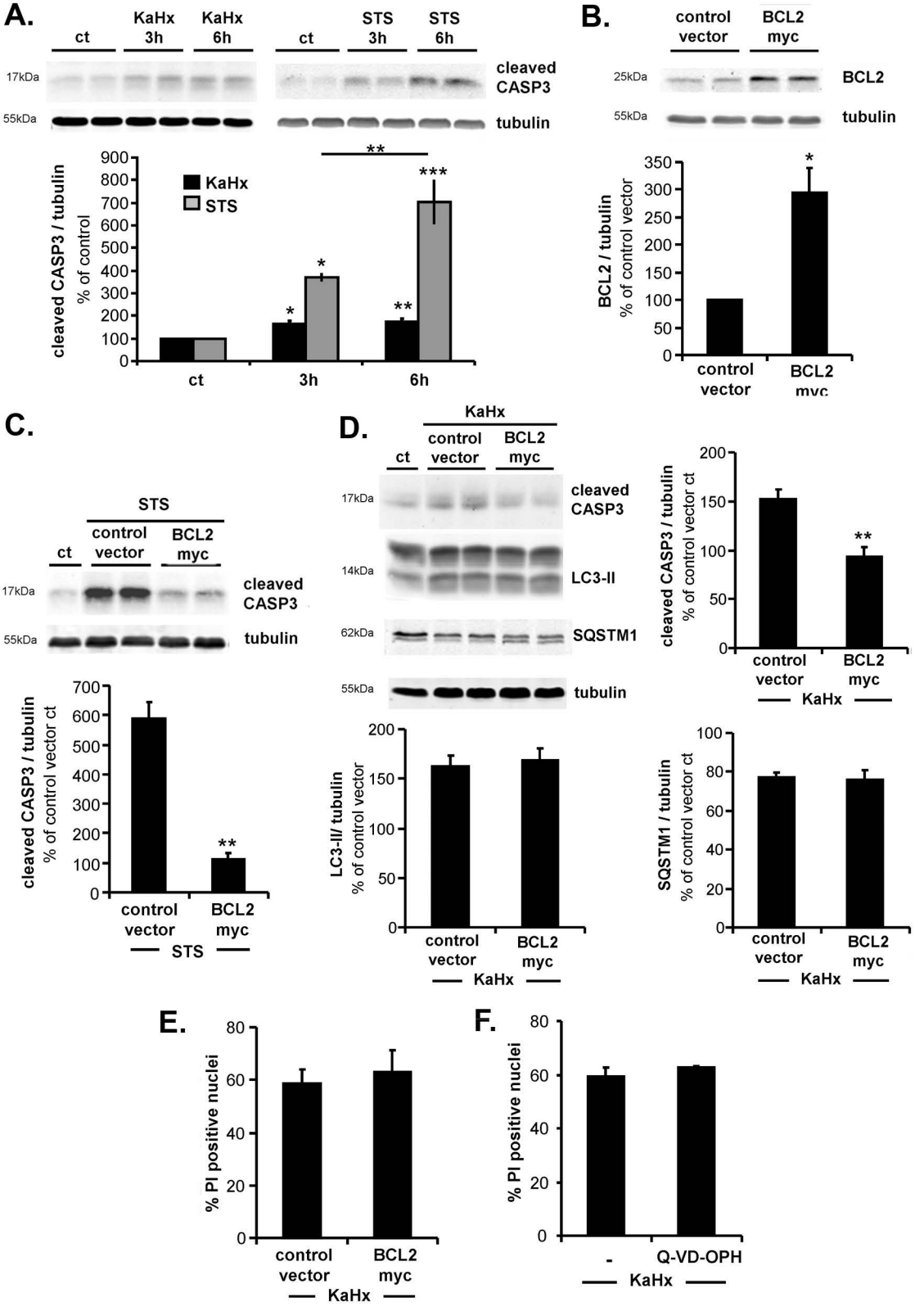
A.
ct
KaHx 3h
KaHx 6h
STS 3h
STS 6h
17kDa
cleaved CASP3
55kDa
tubulin
cleaved CASP3 / tubulin % of control
KaHx
STS
ct
3h
6h
B.
control vector
BCL2 myc
25kDa
BCL2
tubulin
BCL2 / tubulin % of control vector
C.
STS
control vector
BCL2 myc
cleaved CASP3 / tubulin % of control vector ct
D.
KaHx
LC3-II
14kDa
62kDa
SQSTM1
LC3-II/ tubulin % of control vector
SQSTM1 / tubulin % of control vector ct
E.
% PI positive nuclei
F.
Q-VD-OPH

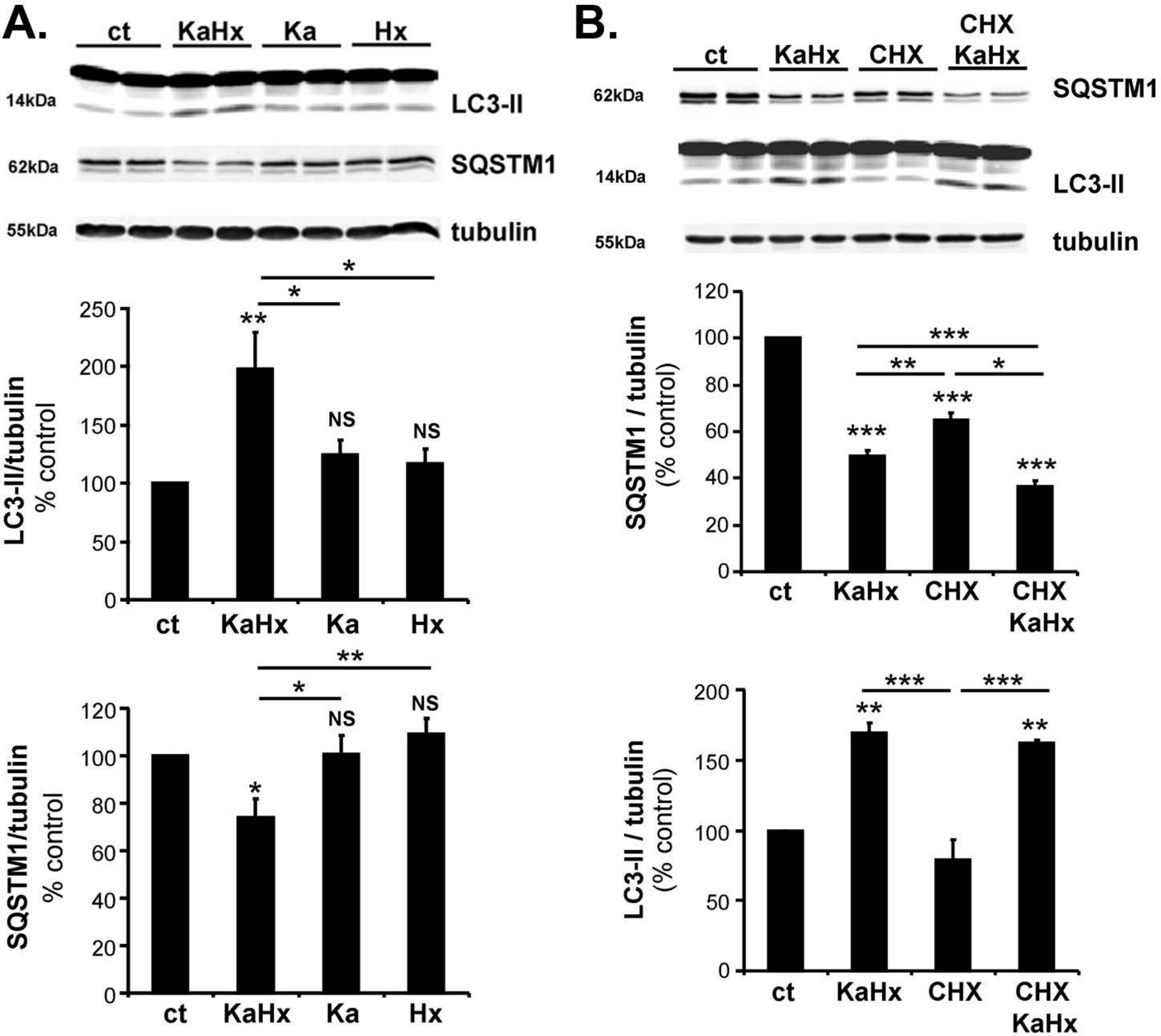
A.
ct
KaHx
Ka
Hx
14kDa
LC3-II
62kDa
SQSTM1
55kDa
tubulin
LC3-II/tubulin
% control
250
200
150
100
50
0
**
*
*
NS
NS
ct
KaHx
Ka
Hx
SQSTM1/tubulin
% control
120
100
80
60
40
20
0
**
*
*
NS
NS
ct
KaHx
Ka
Hx
B.
ct
KaHx
CHX
CHX
KaHx
62kDa
SQSTM1
14kDa
LC3-II
55kDa
tubulin
SQSTM1 / tubulin
(% control)
120
100
80
60
40
20
0
***
**
*
***
***
***
ct
KaHx
CHX
CHX
KaHx
LC3-II / tubulin
(% control)
200
150
100
50
0
***
***
**
**
ct
KaHx
CHX
CHX
KaHx

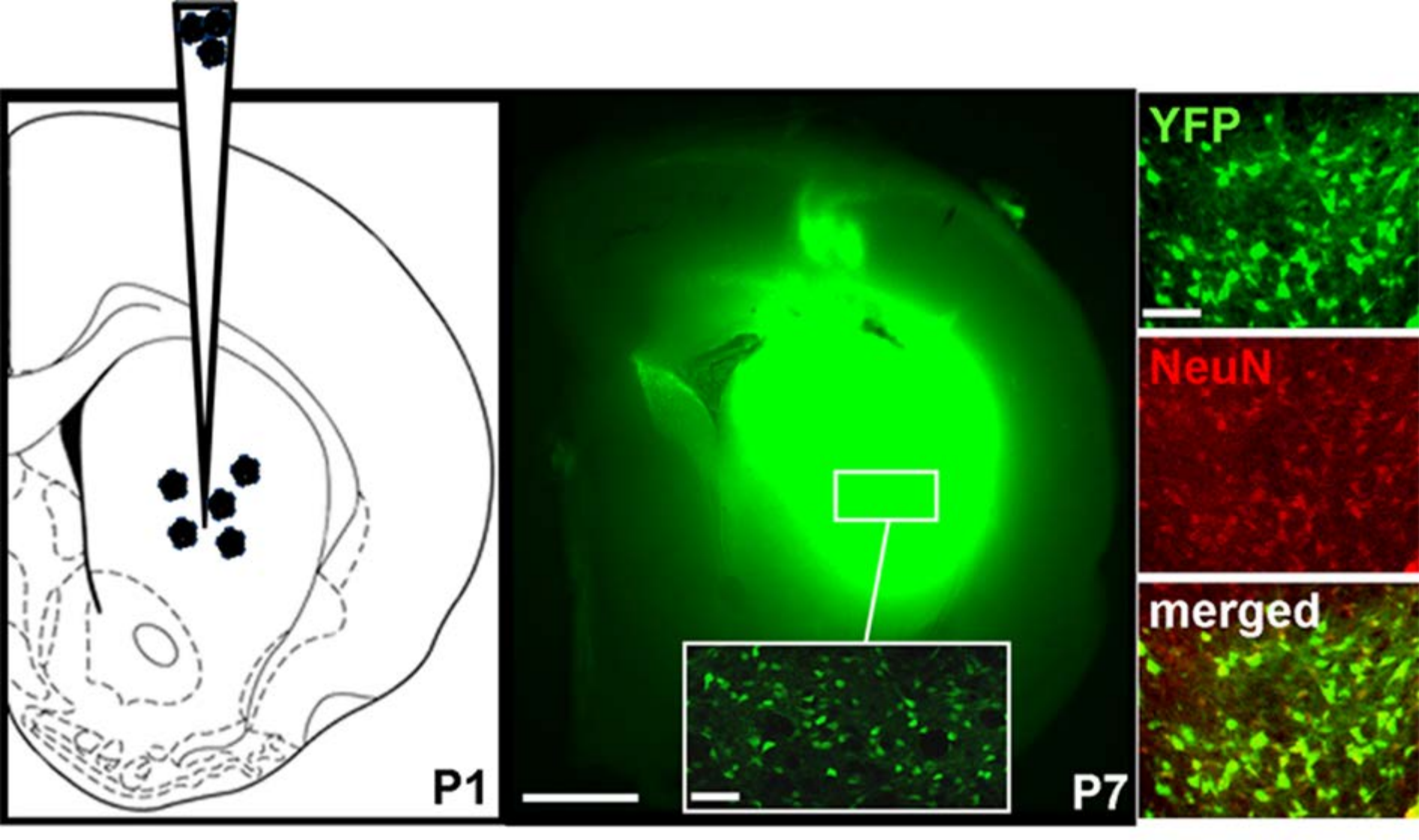
P1
P7
YFP
NeuN
merged

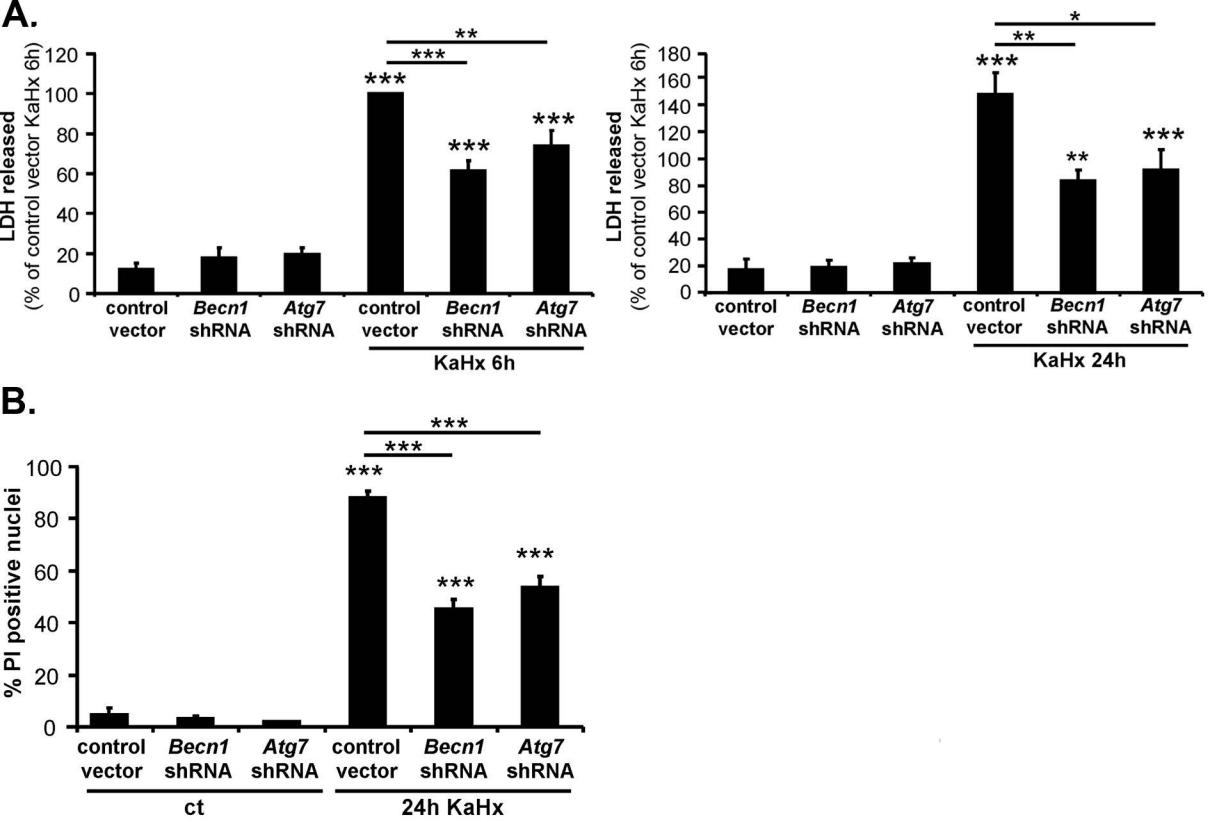
A.
LDH released
(% of control vector KaHx 6h)
120
100
80
60
40
20
0
***
**
***
***
***
control vector
Becn1 shRNA
Atg7 shRNA
control vector
Becn1 shRNA
Atg7 shRNA
KaHx 6h
LDH released
(% of control vector KaHx 6h)
180
160
140
120
100
80
60
40
20
0
*
**
***
**
***
control vector
Becn1 shRNA
Atg7 shRNA
control vector
Becn1 shRNA
Atg7 shRNA
KaHx 24h
B.
% PI positive nuclei
100
80
60
40
20
0
***
***
***
***
***
control vector
Becn1 shRNA
Atg7 shRNA
control vector
Becn1 shRNA
Atg7 shRNA
ct
24h KaHx